Spectroscopic decomposition of the Galactic Ridge X-ray Emission with *Suzaku*

Takayuki YUASA
ASTRO-H Project Researcher, JAXA/ISAS

Kazuo Makishima
Kazuhiro Nakazawa
The University of Tokyo

Publications:
Yuasa, Nakazawa, Makishima et al. 2010, A&A, 520, A25+
Yuasa, Ph.D thesis, The University of Tokyo, 2010

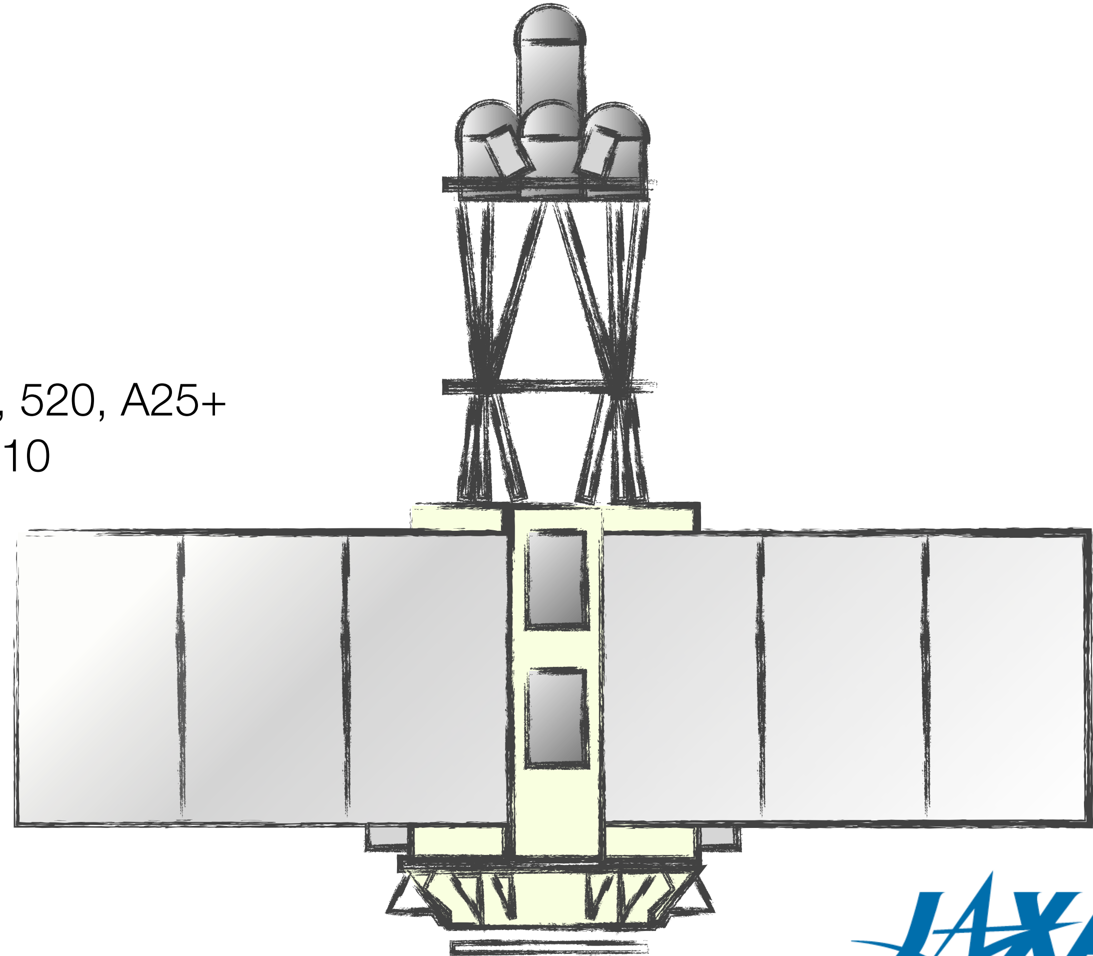

Introduction

Galactic Ridge X-ray Emission (GRXE)

X-ray background emission observed along with the Galactic disk and the Galactic bulge. Total luminosity is ~10^{38} erg/s in 2-10 keV.

The origin of the GRXE has been one of great mysteries in X-ray astrophysics over 40 years (e.g. Cooke et al. 1969).

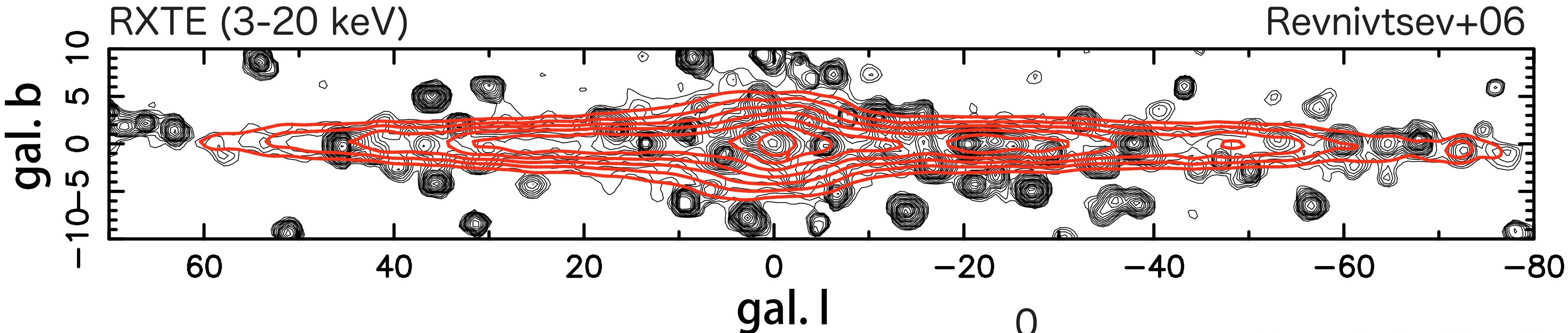

Spectral feature **(e.g. Koyama et al. 1986)**

- Continuum + Emission lines.
- Coexistence of lines from light (Si/S) and heavy (Fe) elements.
  - Multi-temperature plasma?

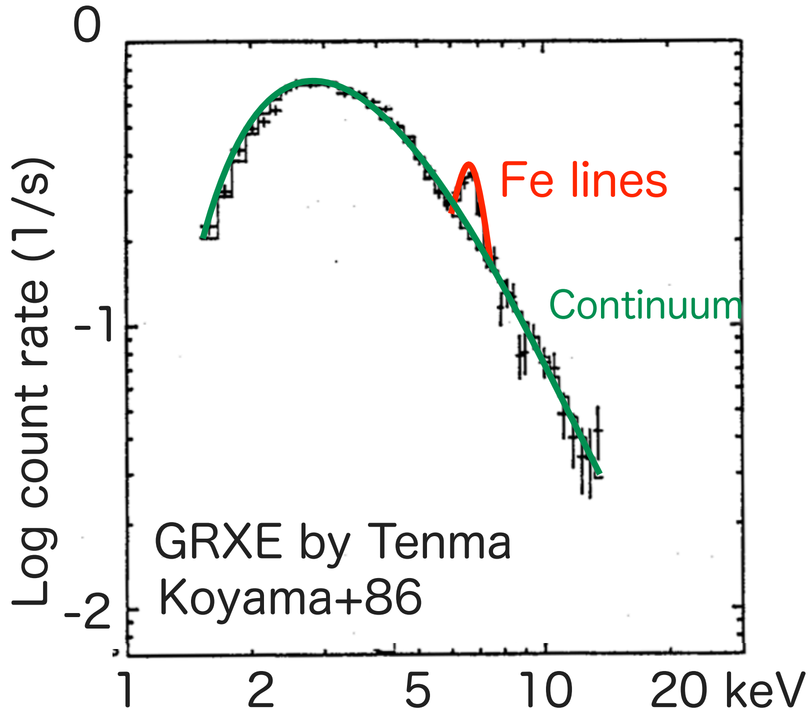

The origin of the GRXE

Chandra 1 Ms image

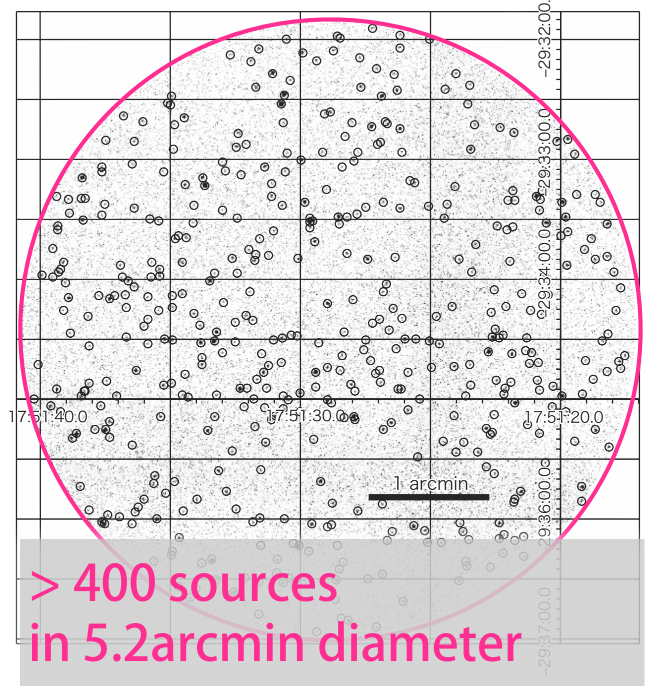

Recent findings from Chandra deep observation

- 80% of detected GRXE flux was resolved into point sources (Revnivtsev+09).
- The GRXE consists of superposition of numerous dim point sources, such as **coronal X-ray sources** and **accreting WDs**.

soft X-ray band   hard X-ray band

Our approach

1. Construct a spectral model of **accreting WDs**, especially **intermediate polars (IPs)**, and then check its validity using data of nearby sources.
   - We concentrate on intermediate polars which have hardest spectra among accreting WDs.
2. Use the IP spectral model to **spectroscopically decompose the GRXE**.

Studies of Magnetic accreting WDs

Modeling a spectrum from an accretion column

Geometry and emission process

- Accreting matter freely falls along the B field lines. Near the WD surface (∼100 km above the surface), gas bulk velocity exceeds the sound velocity.
- A shock stands, and converts bulk kinematic energy into internal energy. The heated gas cools in the post-shock region (PSR) via optically thin-thermal X-ray emission.
- Equating conservation laws leads to density, temperature, and velocity profiles in the PSR.

$$\frac{\mathrm{d}}{\mathrm{d}z}(\rho v) = 0, \qquad \frac{\mathrm{d}}{\mathrm{d}z}(\rho v^2 + P) = -\frac{GM_{\mathrm{WD}}}{z^2}\rho\,,$$

$$v\frac{\mathrm{d}P}{\mathrm{d}z} + \gamma P\frac{\mathrm{d}v}{\mathrm{d}z} = -(\gamma - 1)\underline{\Lambda n^2}$$

thin-thermal cooling function
(e.g. Schure+09)

- The system reduces to an initial value problem of ODEs (Cropper+99, Suleimanov+05).
- Example of the M_{WD}=0.7 M_{sun} case.

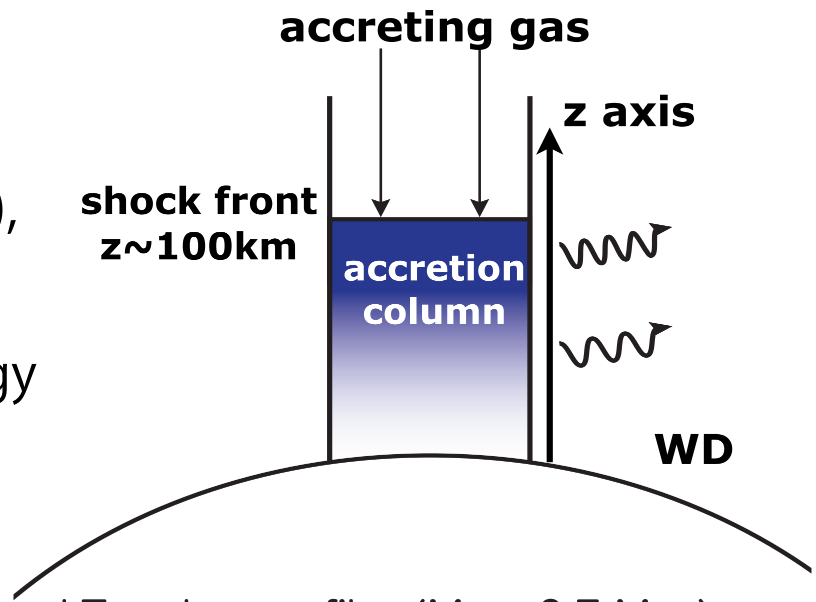

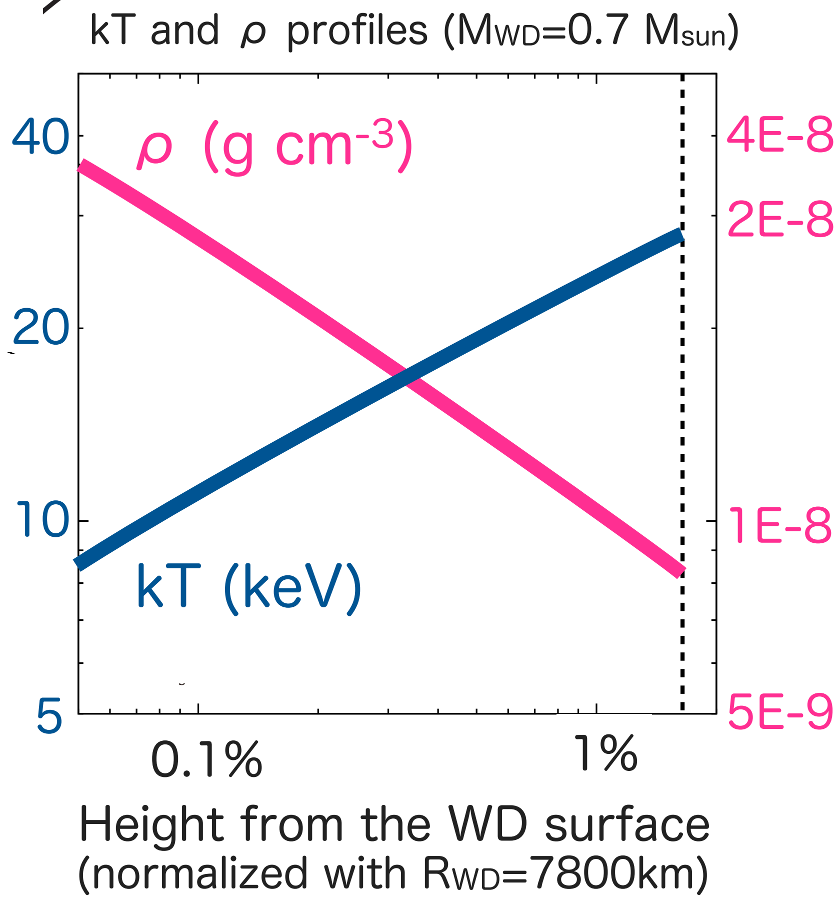

Construct a total spectrum

- APEC was convolved with the emissivity to produce a total spectrum. Thus, the model consists of multi-temperature emission.
- **M_{WD}** and **Fe abundance** are primary parameters of the model.
  - Updates from previous studies : emission lines + variable metal abundance
- Heavier masses result harder spectra, i.e. cutoff energy ∝ shock temp ∝ WD mass
- By fitting observed spectra, WD mass can be estimated.
  - Cutoff energy and Fe line ratio are important factors constraining the mass.

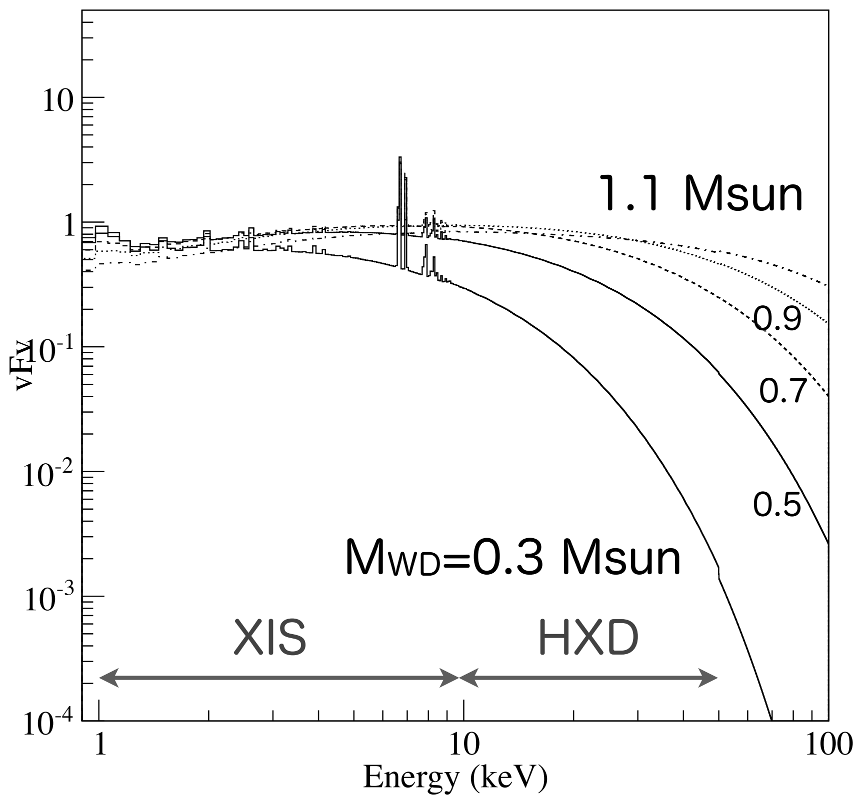

Construct a total spectrum

- APEC was convolved with the emissivity to produce a total spectrum. Thus, the model consists of multi-temperature emission.
- **M_{WD}** and **Fe abundance** are primary parameters of the model.
    - Updates from previous studies : emission lines + variable metal abundance
- Heavier masses result harder spectra, i.e. cutoff energy ∝ shock temp ∝ WD mass
- By fitting observed spectra, WD mass can be estimated.
    - Cutoff energy and Fe line ratio are important factors constraining the mass.

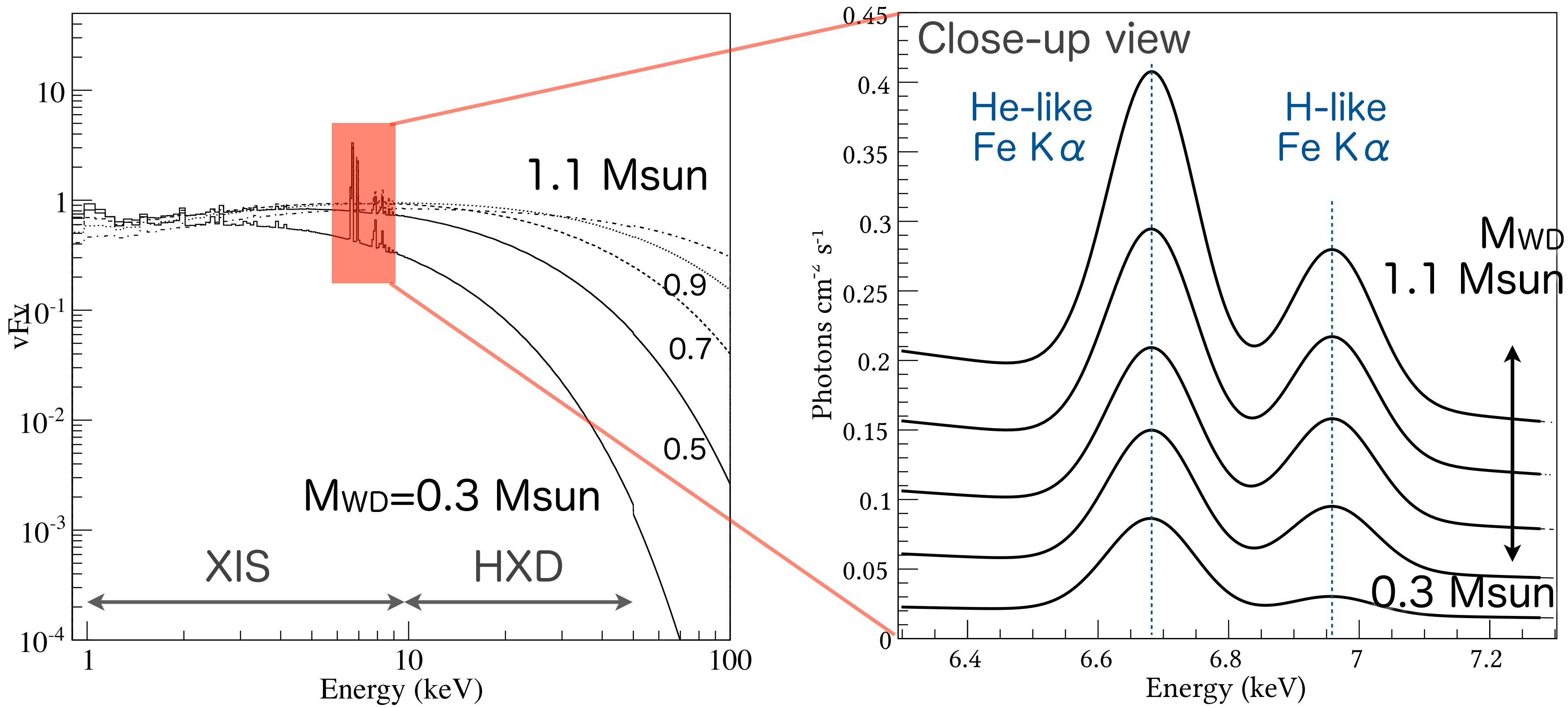

Spectral fitting with near-by IPs (Yuasa+10, A&A)

- The XIS clearly resolves three Fe lines. The HXD detects signals up to 40-50 keV.
- Single kT model (apec) → Fe lines and continuum **inconsistent.**
- The IP model successfully reproduced overall spectra and the Fe line structure.
  Note：In the present study the 6.4-keV Fe line was arbitrarily modeled using a Gaussian.

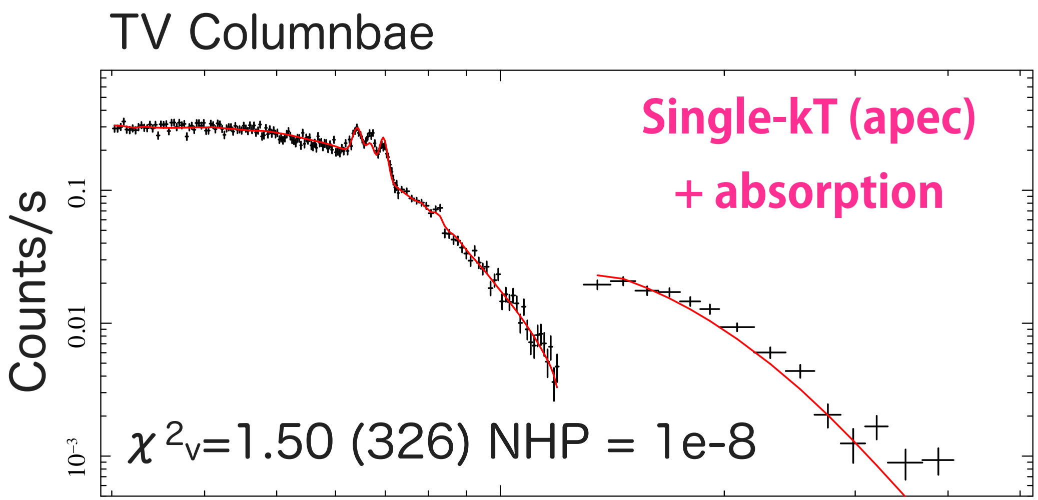

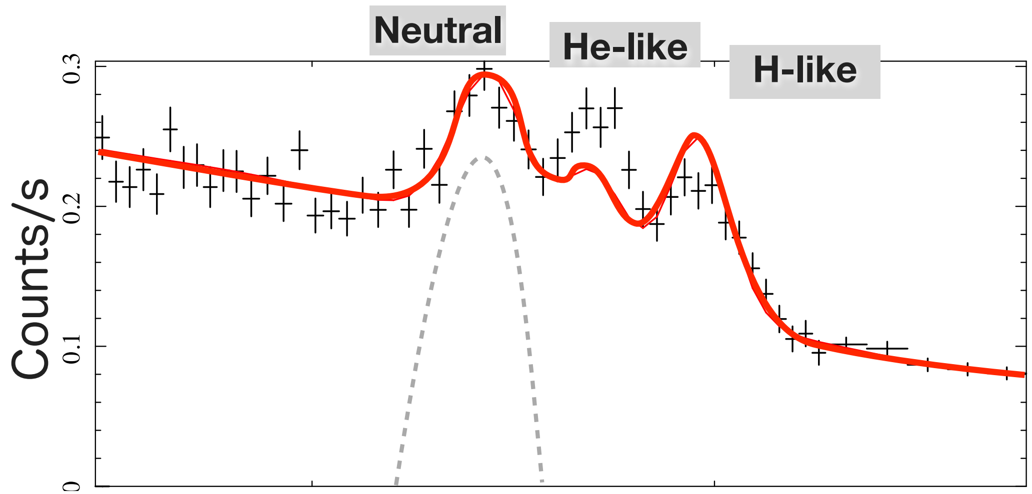

Spectral fitting with near-by IPs (Yuasa+10, A&A)

- The XIS clearly resolves three Fe lines. The HXD detects signals up to 40-50 keV.
- Single kT model (apec) → Fe lines and continuum **inconsistent.**
- The IP model successfully reproduced overall spectra and the Fe line structure.

Note：In the present study the 6.4-keV Fe line was arbitrarily modeled using a Gaussian.

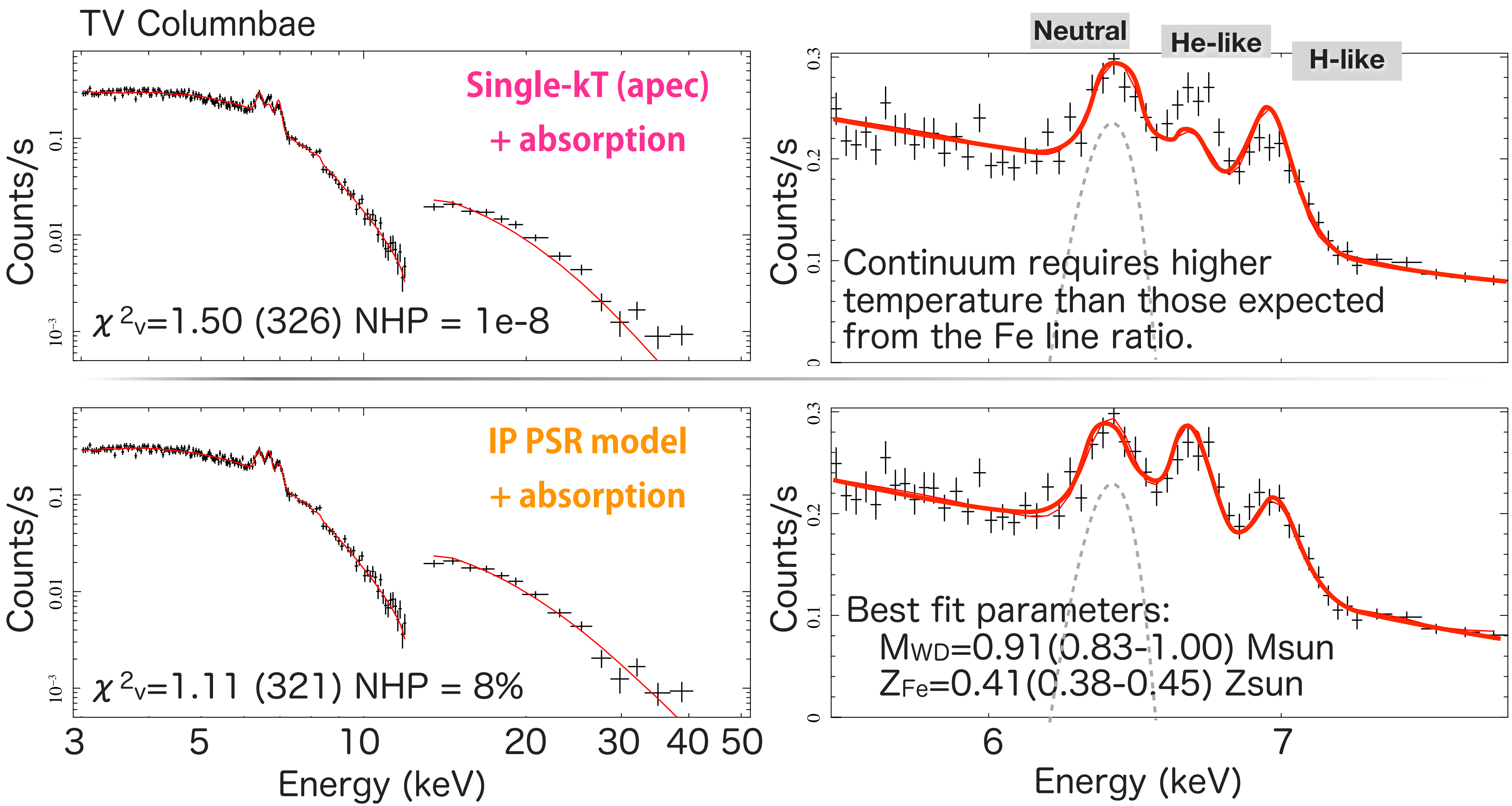

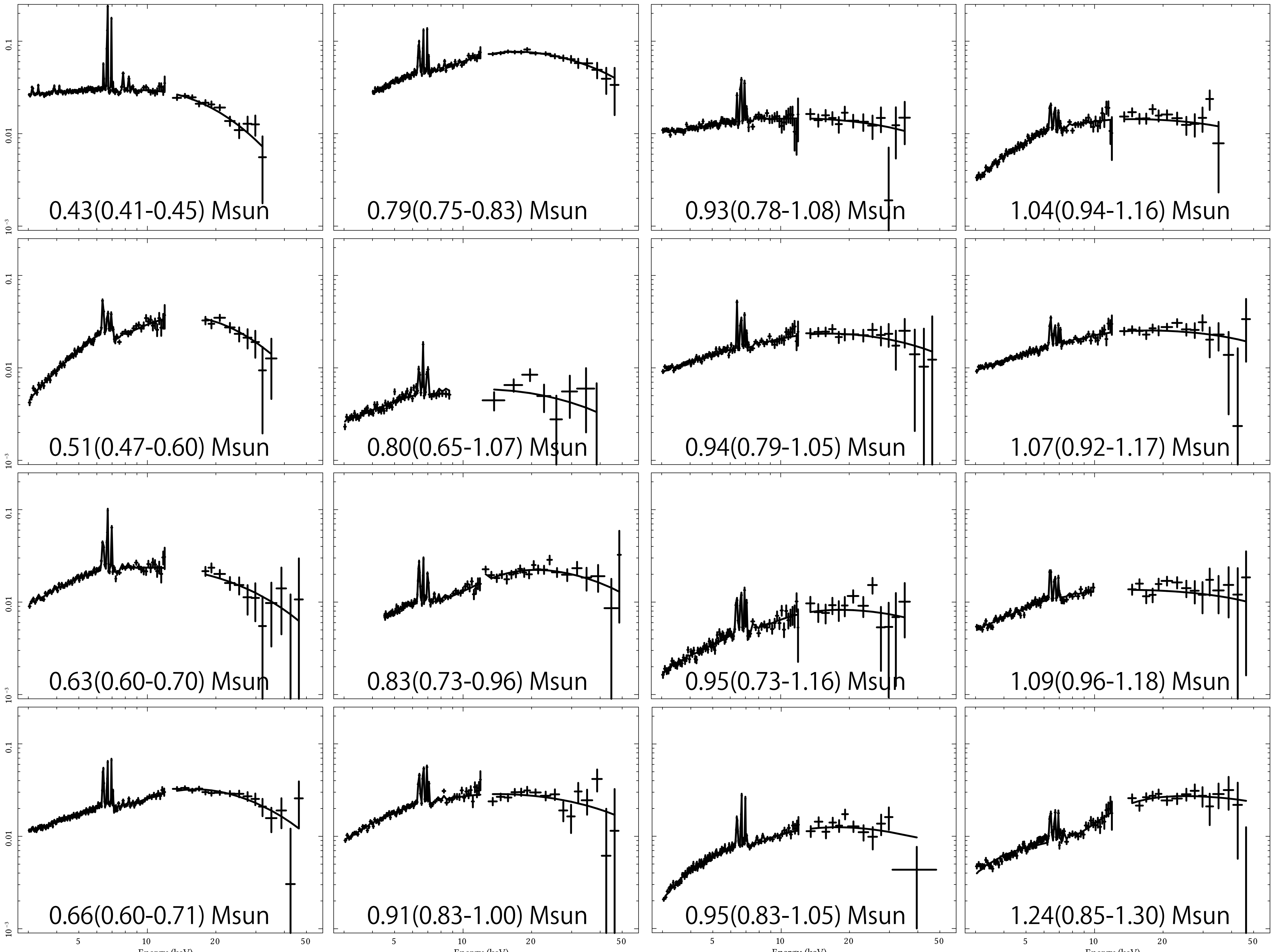
0.43(0.41-0.45) Msun
0.79(0.75-0.83) Msun
0.93(0.78-1.08) Msun
1.04(0.94-1.16) Msun
0.51(0.47-0.60) Msun
0.80(0.65-1.07) Msun
0.94(0.79-1.05) Msun
1.07(0.92-1.17) Msun
0.63(0.60-0.70) Msun
0.83(0.73-0.96) Msun
0.95(0.73-1.16) Msun
1.09(0.96-1.18) Msun
0.66(0.60-0.71) Msun
0.91(0.83-1.00) Msun
0.95(0.83-1.05) Msun
1.24(0.85-1.30) Msun

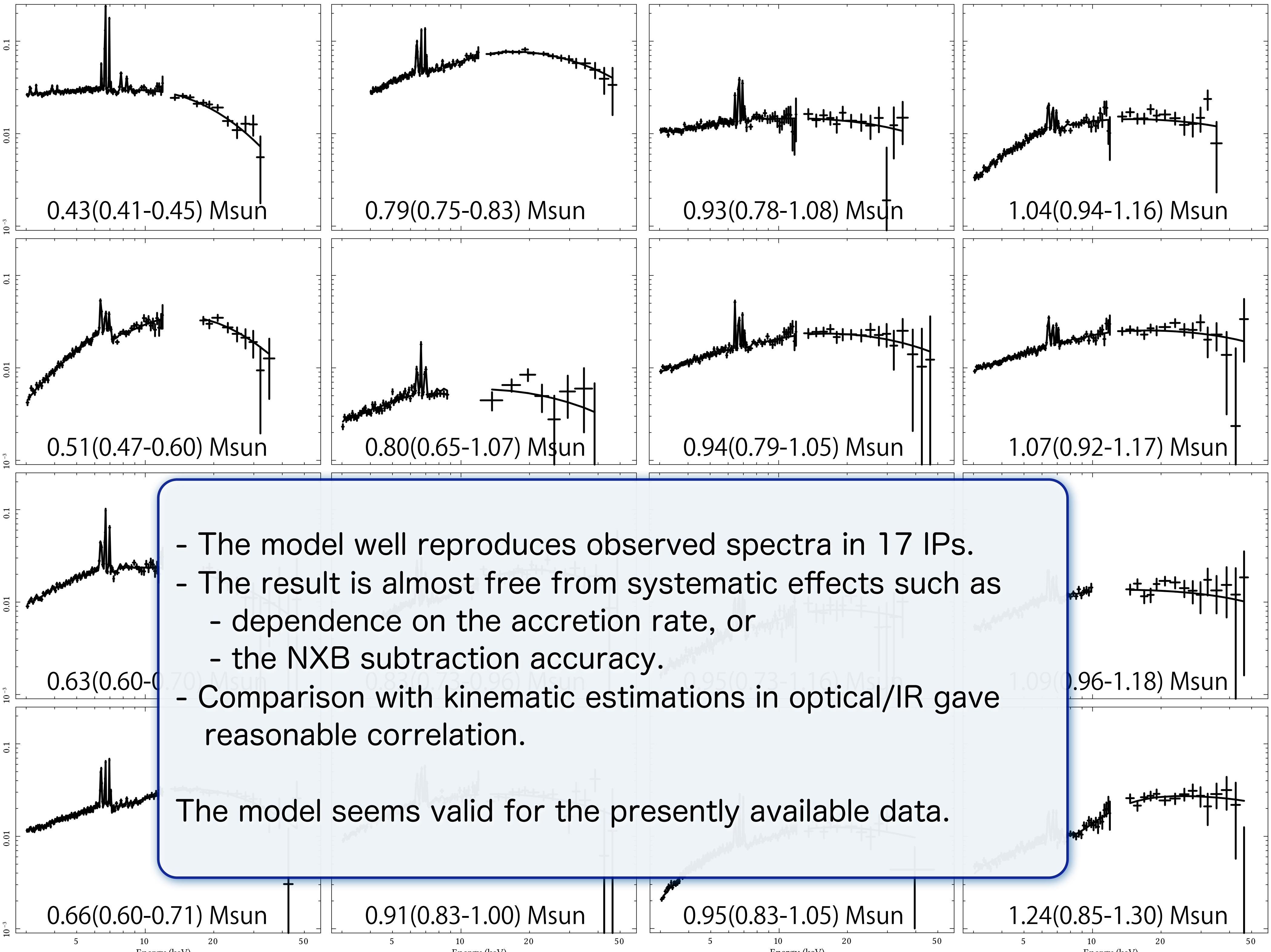

- The model well reproduces observed spectra in 17 IPs.
- The result is almost free from systematic effects such as
  - dependence on the accretion rate, or
  - the NXB subtraction accuracy.
- Comparison with kinematic estimations in optical/IR gave reasonable correlation.

The model seems valid for the presently available data.

Spectral analysis of the GRXE

Suzaku GRXE observations

- By summing observations around the Galactic center region, we constructed data set of the GRXE (avoiding known bright X-ray sources).
- Region 1 = 590 ks; Region 2 = 420 ks → Total exposure = 1Ms

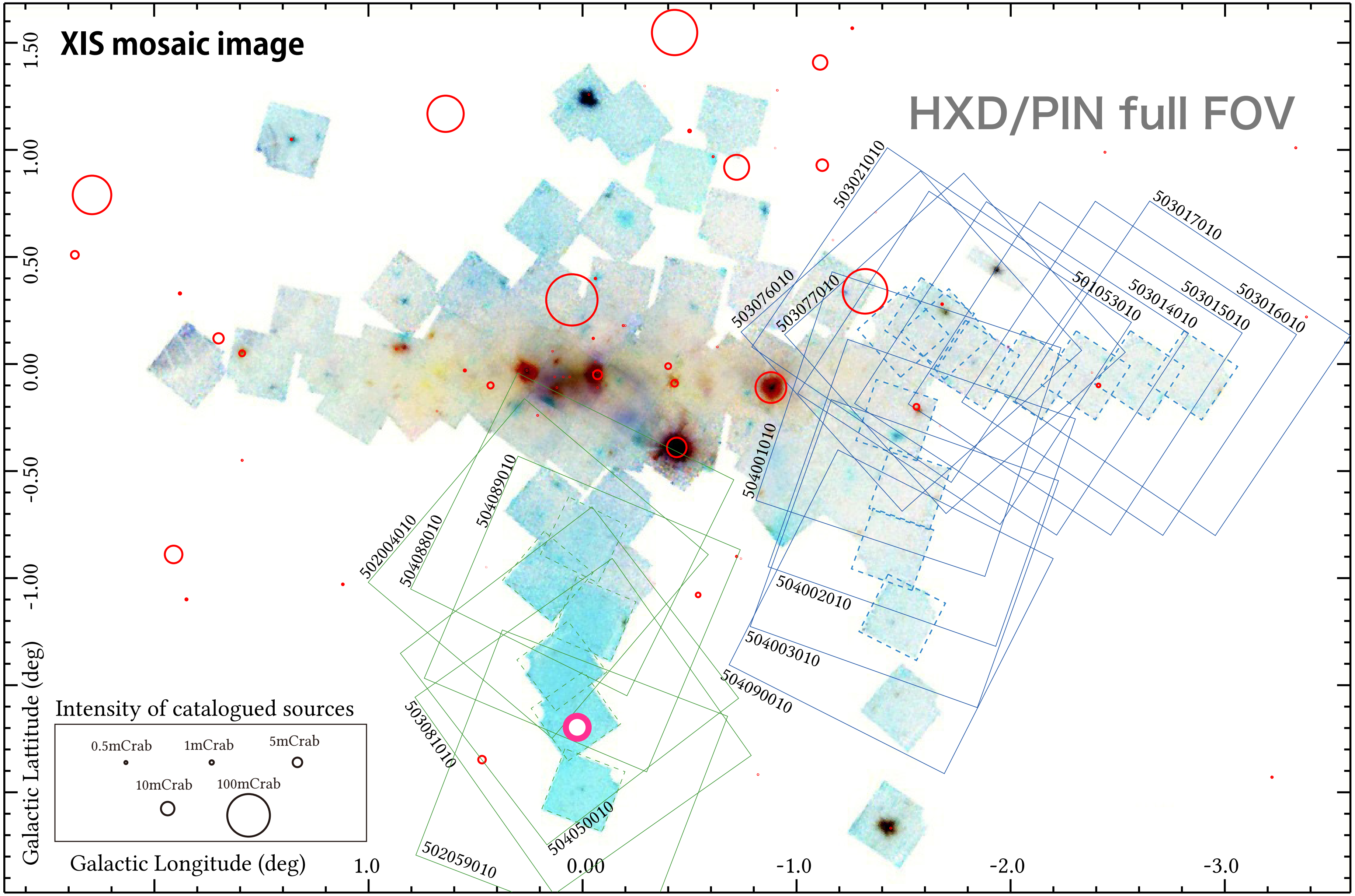

Suzaku GRXE observations

- By summing observations around the Galactic center region, we constructed data set of the GRXE (avoiding known bright X-ray sources).
- Region 1 = 590 ks; Region 2 = 420 ks → Total exposure = 1Ms

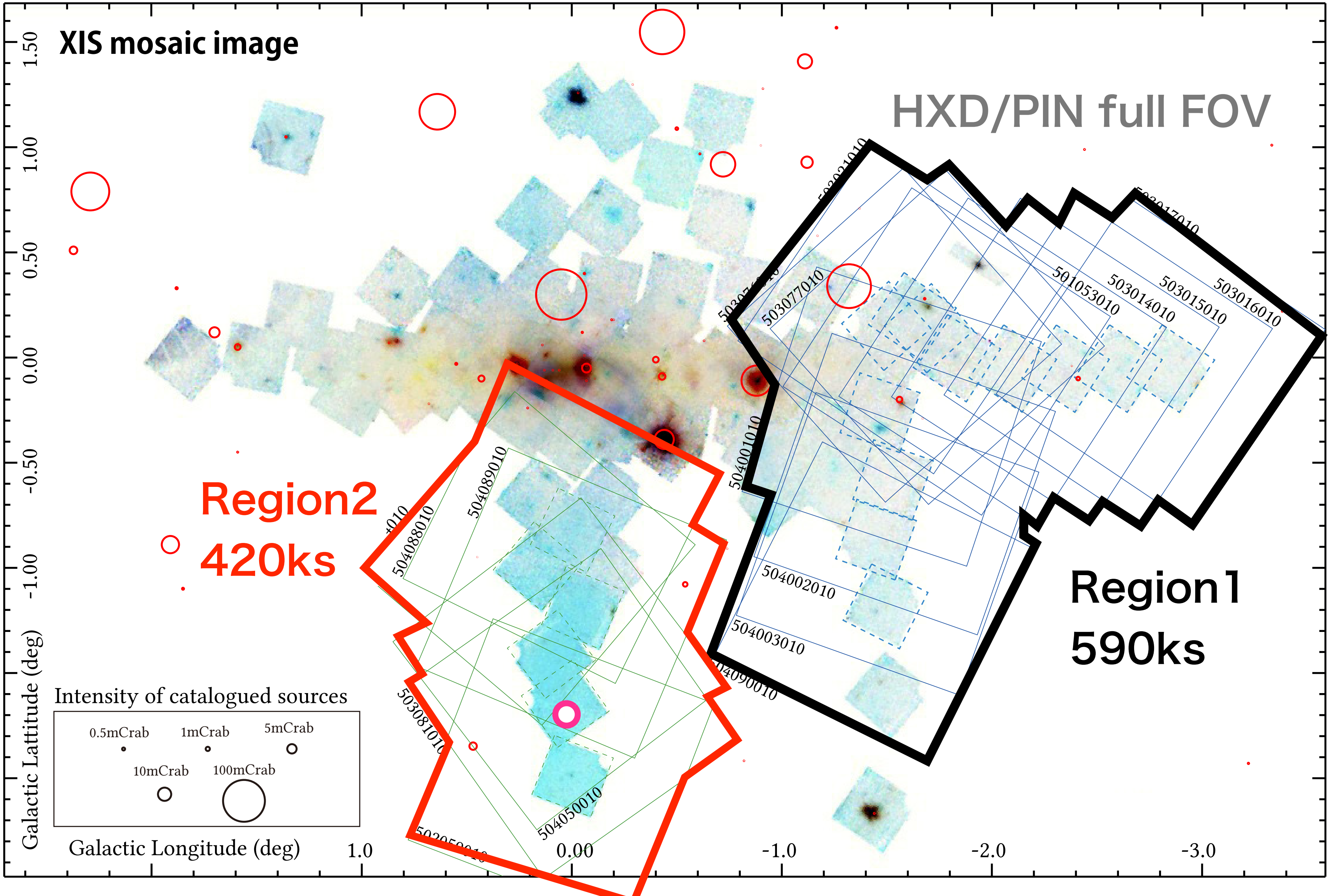

Close-up view of the XIS spectrum

- Lines from lighter (S/Ar/Ca) elements coexist with those from Fe (reconfirmation of Ebisawa+08 with much higher statistics).
- This strongly indicates contributions from thermal emissions with different temperatures.
- At least two distinct plasma temperatures are necessary to reproduce the spectrum.

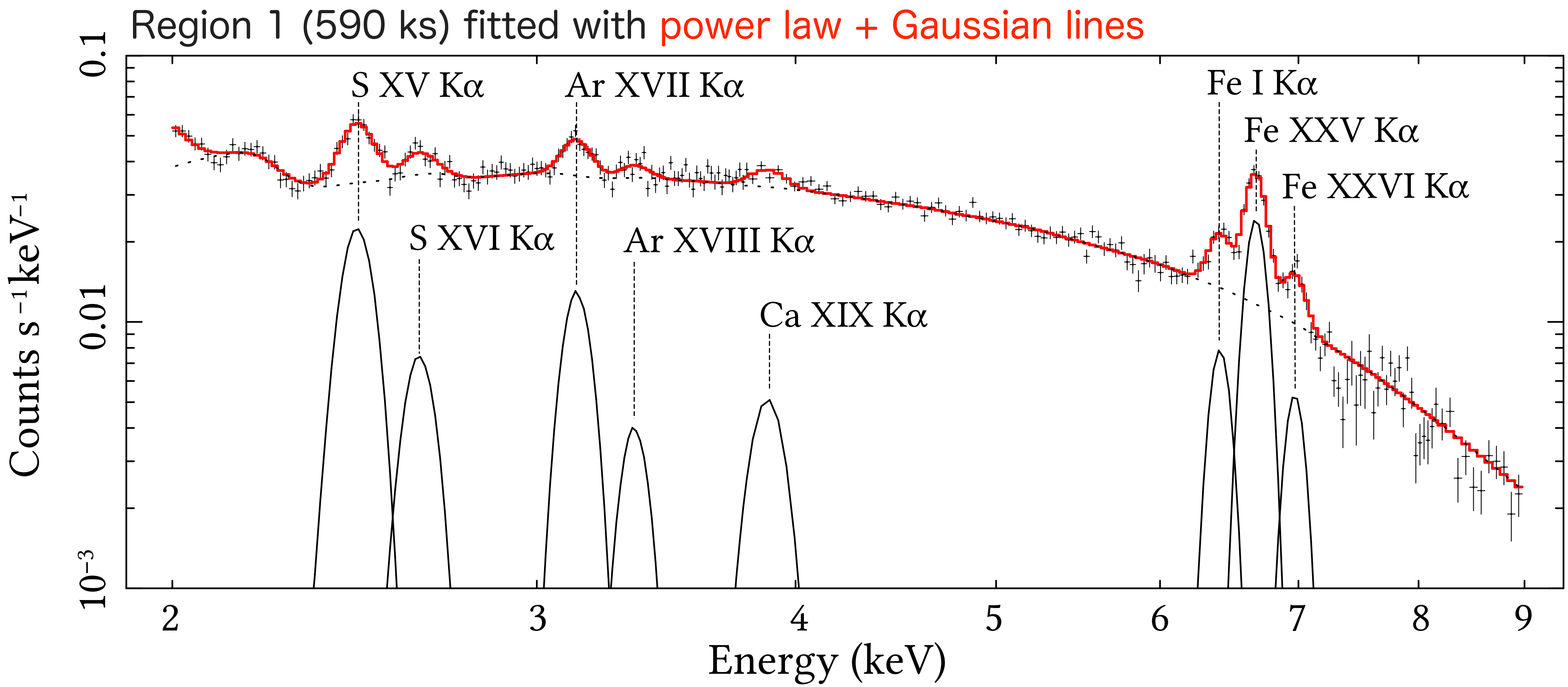

Fitting the GRXE in the hard X-ray band

- A power-law model gives a soft index, **Γ =2.8±0.2**, and extrapolation of this to lower energies contradicts with the XIS spectrum.
- Single-temperature thermal model gave the best fit at **kT=15.7 (13.7-18.4) keV**.
- The IP spectral model well reproduced the data with **M_{WD}=0.66 (0.59-0.75) M_{Sun}.**
  - This could be interpreted as a representative WD mass of IPs in the Galaxy. (c.f. ～0.5 M_{Sun} by Krivonos+07 with INTEGRAL data)

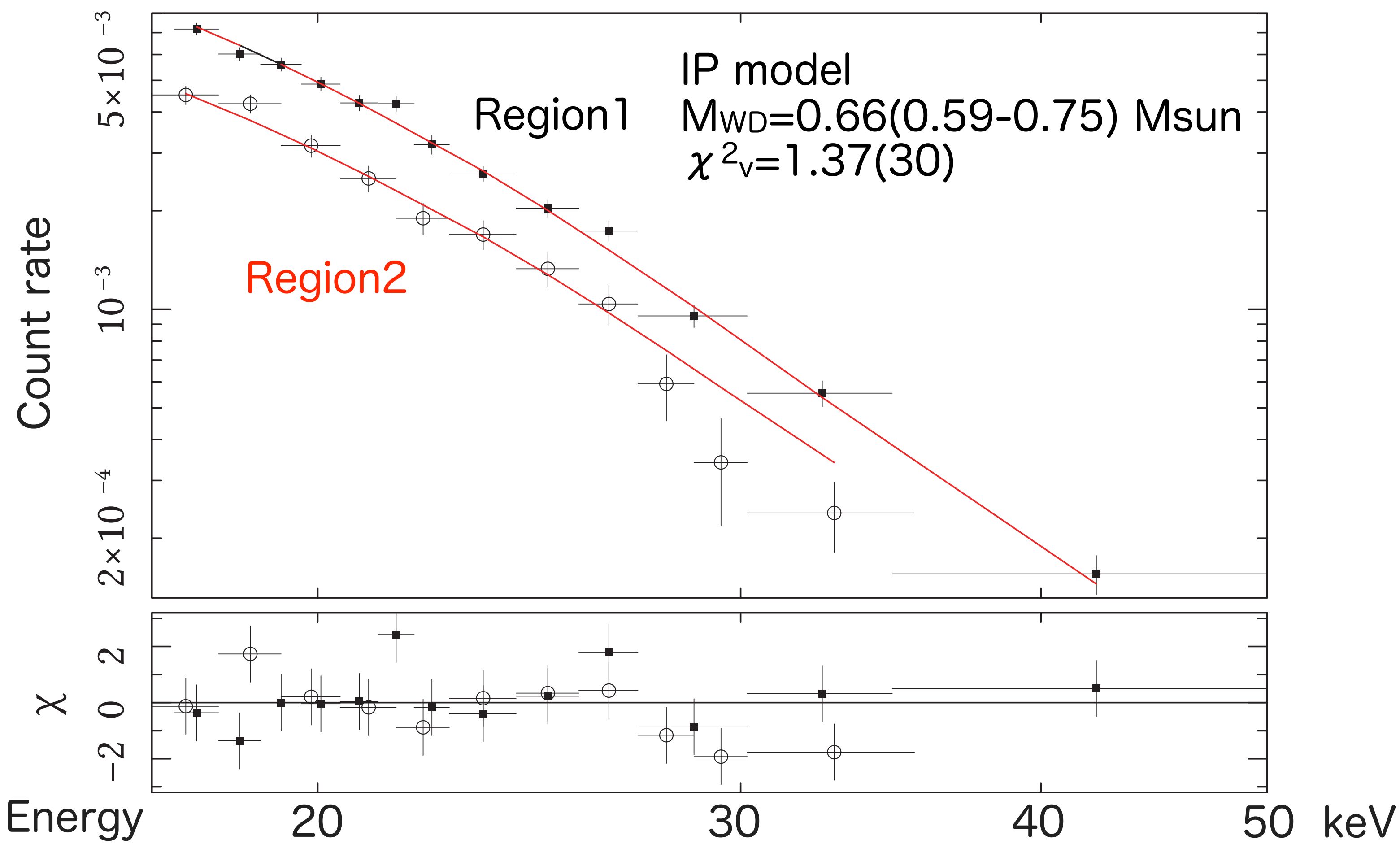

Broad-band decomposition

Fit with the IP PSR model + single-kT thermal model.
(1) M_{WD} was fixed at the HXD result.

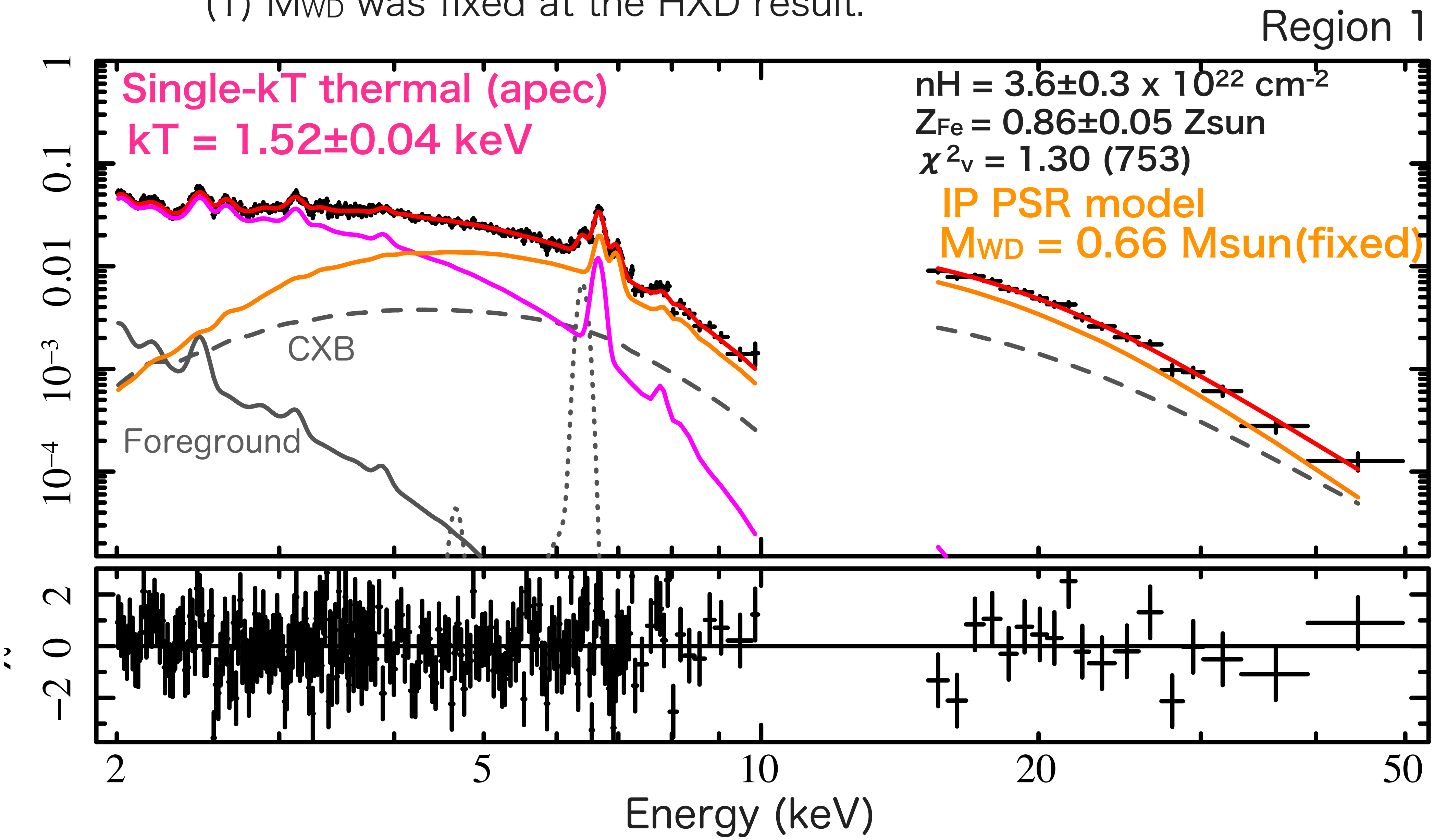

Broad-band decomposition

Fit with the IP PSR model + single-kT thermal model.
(2) M_{WD} was allowed to freely vary.

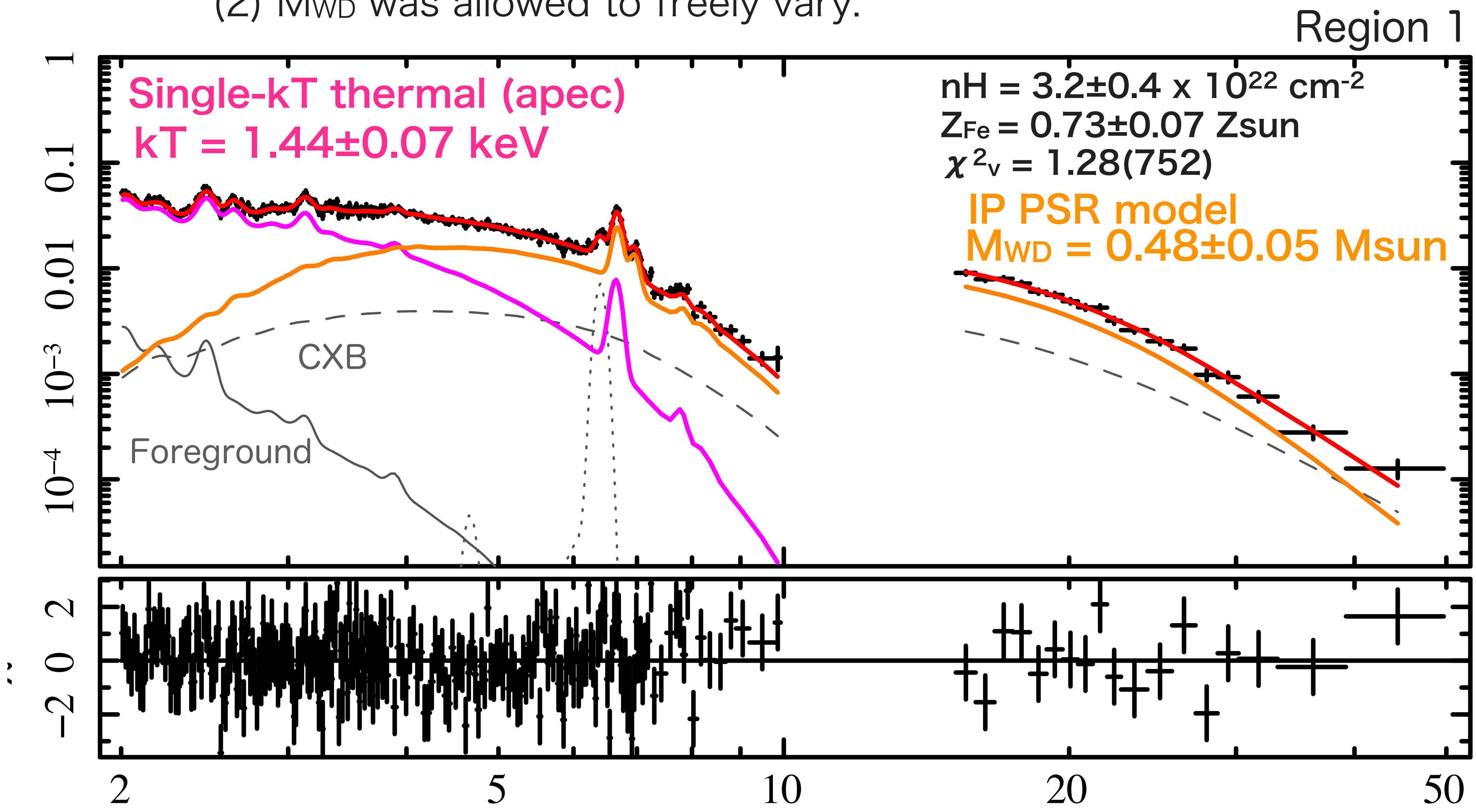

low-kT component ～1-1.5 keV → typical to coronal sources (active binary stars)

high-kT component～>10 keV → well reproduce by the IP model

Summary of results

- An X-ray spectral model for IPs was constructed, and its validity was confirmed by applying it to Suzaku spectra of 17 nearby IPs. WD mass estimates were obtained as byproducts.

- Broad-band GRXE spectra (2-50 keV) were extracted from 1-Ms Suzaku data.
  - Hard X-ray spectrum was well reproduced with the IP spectral model.
  - The temperature of the low-kT component is consistent with typical temperature of coronal sources such as active binary stars.

Conclusion

The present study precisely measured the GRXE spectrum over 1-50 keV, and decomposed it into to distinctive components which have physical counterparts such as active binary stars and accreting WD binaries.

Being complementary to the imaging result, this result also supports the point source scenario as the origin of the GRXE.

LogN-LogS of required point sources will be available in Q&A session.

Broad-band GRXE spectra

- Spectra of individual pointings were very similar within Regions 1 and 2.
- To increase statistics, we added data in each Region.
- We obtained a significant signals up to 50 keV.
- Three Fe emission lines were clearly detected together with those from S/Ar.

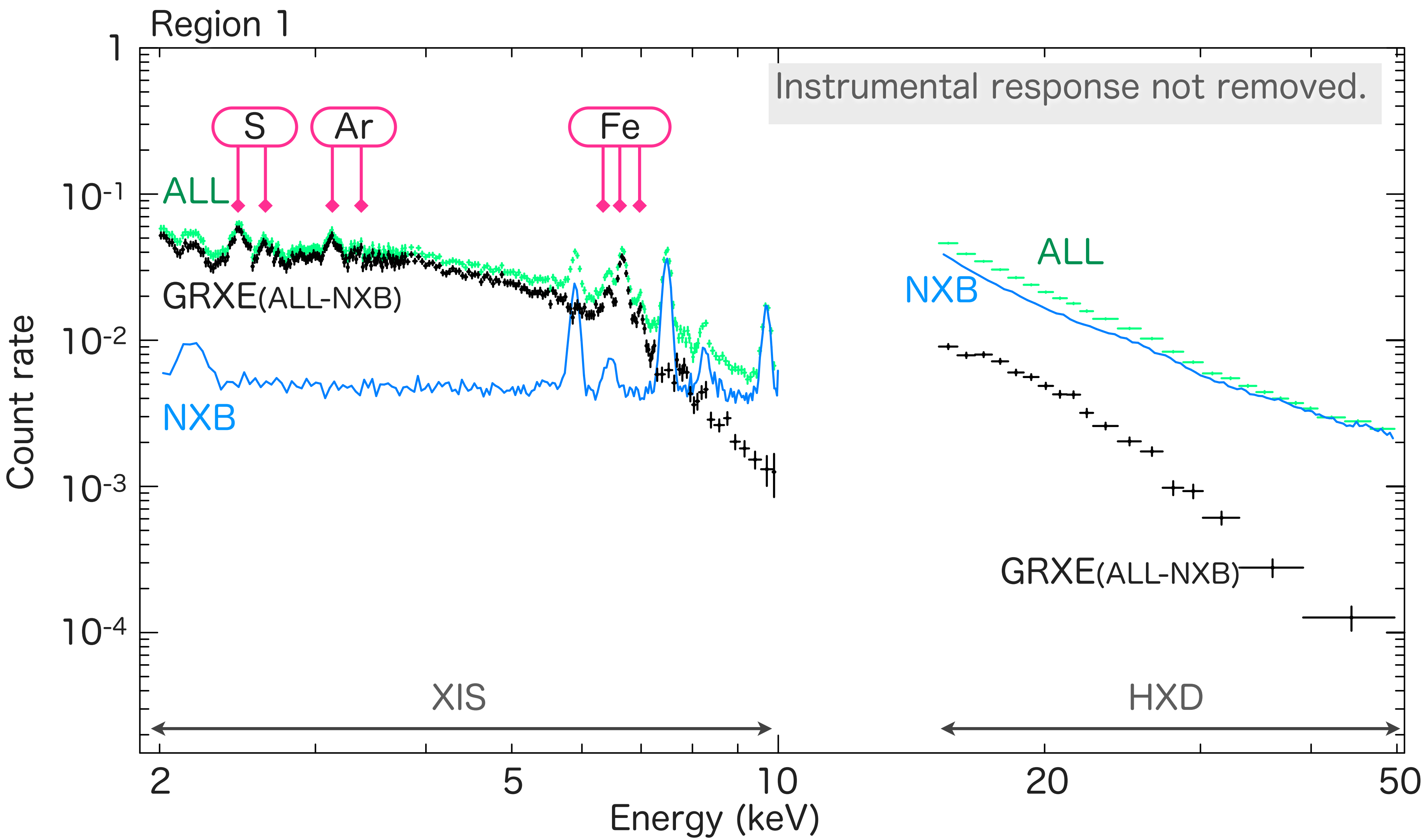

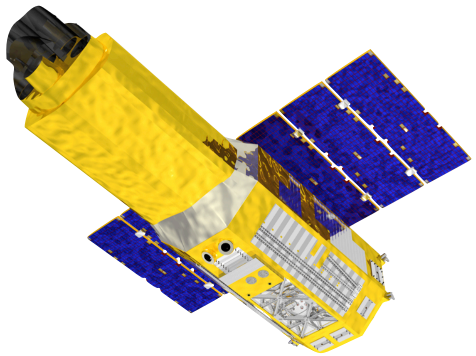

The Suzaku X-ray satellite

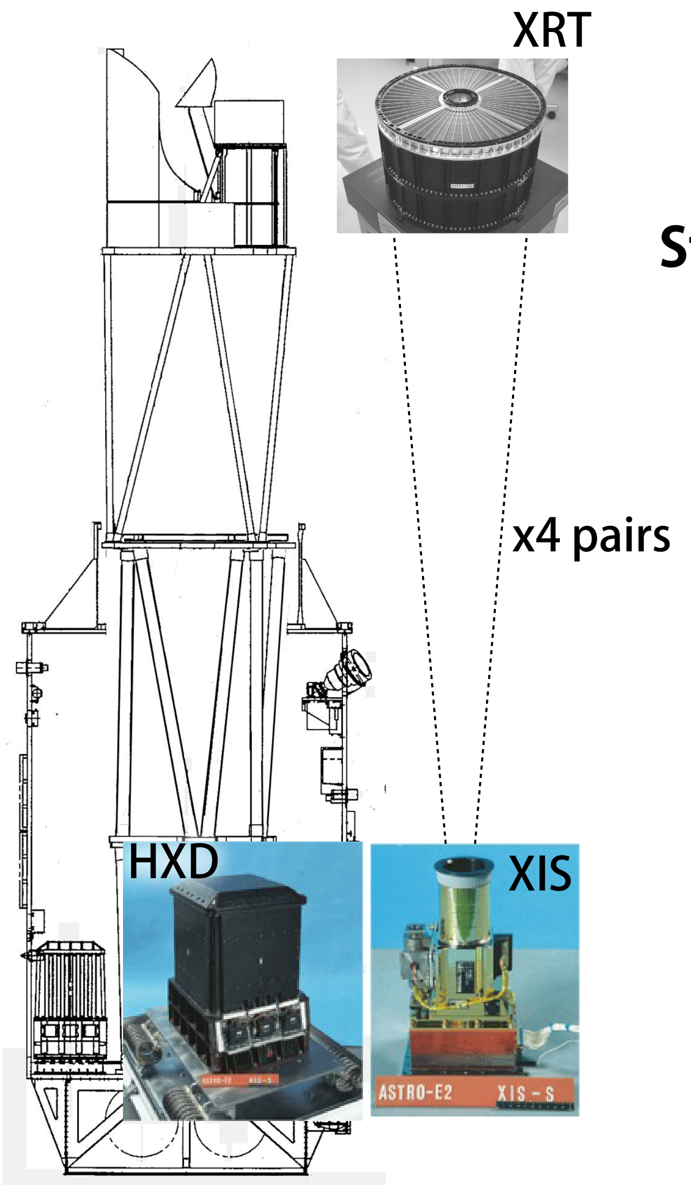

Overview

- Launched in July 2005, and still operational.
- Orbiting the low Earth orbit (alt. of ~550km).
- More than 1500 sets of public data as of May 2011.

Strong points

- X-ray CCD XIS + X-ray mirror XRT, and Hard X-ray Detector (HXD) provide a wide-band energy coverage over **0.5-600 keV**.
- **High energy resolution of ∼150-200 eV** below 10 keV.

Our study is the first GRXE study that **simultaneously**
(1) resolves emission lines from multiple elements,
(2) accurately measures the hard X-ray spectral shape,
using detectors well calibrated each other.

Accreting white dwarfs
(Cataclysmic Variable; CV)

- Mass of a companion star is transferred via the Roche lobe.
- It accretes onto a white dwarf
  - creating an accretion disk (weak B)
  - channeled by the magnetic field (strong B)
- White dwarf occupies ~10% of the stellar mass in the Galaxy, and binaries are ubiquitous.
- dot{M}$\sim 10^{-11\text{--}9}$ Msun/yr.
- L$\sim$(GR$_{WD}$dot{M})/R$_{WD}$$\sim 10^{31\text{-}34}$ erg/s.
- **Low luminoisty & numerous**
  → candidate of the GRXE origin
- $\sim$10% has strong B filed ($10^{5\text{-}9}$ G).

Magnetic CV

- Polar ($10^{7\text{-}9}$ G)
  and **Intermediate Polar** (**IP**; $10^{5\text{-}7}$ G)
- Hard X-rays are emitted from accretion column on top of the magnetic pole(s):
  continuum + intense Fe lines (similar to the GRXE)

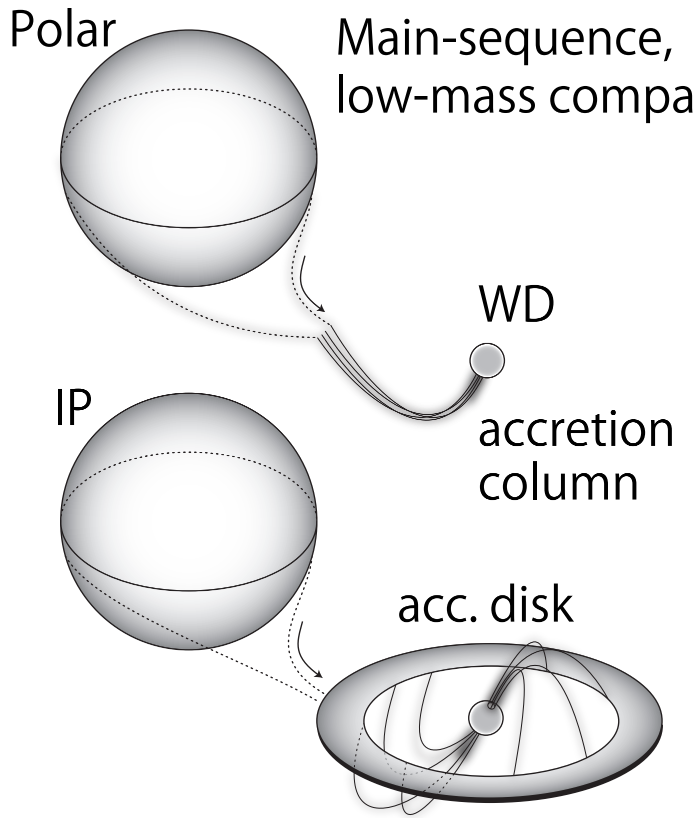

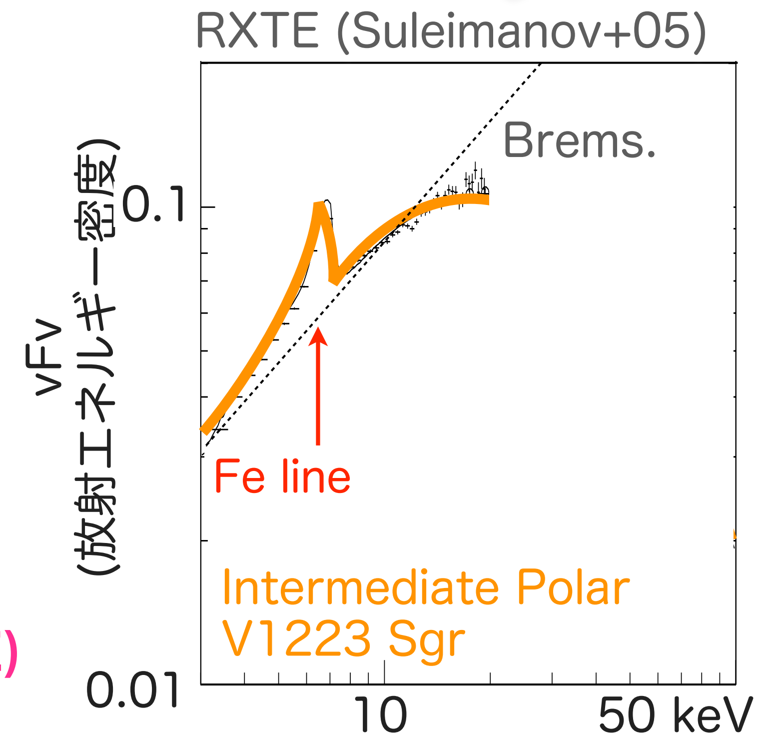

Application to Suzaku IP spectra (Yuasa+10, A&A)

- The model was converted to the local model of XSPEC.
- We check the validity of the model by applying it to actual data.
- Suzaku has been observing ~20 hard X-ray emitting (nearby) IPs as of 2011.
- 17 sources, which give enough signals in the HXD, were selected in this study.
  - This is because the hard X-ray spectrum contains essentially important information on the PSR (i.e. shock temp.)
- The 17 sources cover about 80% of the hard X-ray flux limited IP samples by Swift (Brunschweiger+09).

System	Coordinate[a] RA	Dec	Start time UT	Exp.[b] ks
FO Aquarii	334.481	-8.351	2009-06-05 08:14	33.4
XY Arietis	44.036	19.442	2006-02-03 23:02	93.6
MU Camelopadalis	96.318	73.578	2008-04-14 00:55	50.1
BG Canis Minoris	112.871	9.94	2009-04-11 12:11	45.0
V709 Cassiopeiae	7.204	59.289	2008-06-20 10:24	33.3
TV Columbae	82.356	-32.818	2008-04-17 18:00	30.1
TX Columbae	85.834	-41.032	2009-05-12 16:19	51.1
YY Draconis	175.896	71.703	2008-06-15 18:37	27.4
PQ Geminorum	117.822	14.74	2009-04-12 13:46	43.2

System	Coordinate[a] RA	Dec	Start time UT	Exp.[b] ks
EX Hydrae	193.107	-29.249	2007-07-18 21:23	91.0
NY Lupi	237.061	-45.478	2007-02-01 15:17	86.8
V2400 Ophiuchi	258.146	-24.247	2009-02-27 11:42	110
AO Piscium	343.825	-3.178	2009-06-22 11:50	35.6
V1223 Saggitarii	283.759	-31.163	2007-04-13 11:31	46.2
RX J2133.7+5107	323.432	51.124	2006-04-29 06:50	62.8
IGR J17303-0601	262.59	-5.993	2009-02-16 10:09	27.7
IGR J17195-4100	259.898	-41.015	2009-02-18 11:03	26.9

Two INTEGRAL IPs (Butters+08, Gänsicke+05)

Construct a total spectrum

- Each layer of the PSR → single-kT thermal emission.
- Convolution of the emissivity (kT and ρ) and the single-kT spectrum
  ⇒ total spectrum of the PSR (**multi-kT emission**)
- Heavier masses result harder spectra.
  i.e. cutoff energy ∝ shock temp. ∝ WD mass
- **M_{WD}** and **Fe abundance** are the free parameters of the model (+ normalization).
- By fitting observed spectra, WD mass can be estimated.
  - cutoff energy and Fe line ratio are important there.

Updates from previous studies
- emission lines
- free Fe abundance

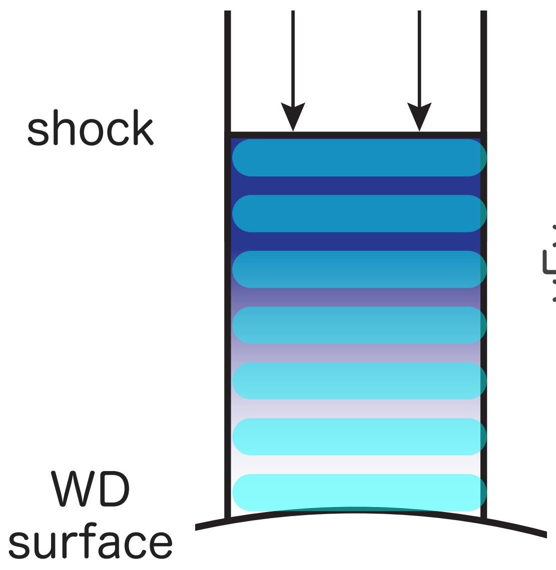

Example of M_{WD}=0.7 Msun

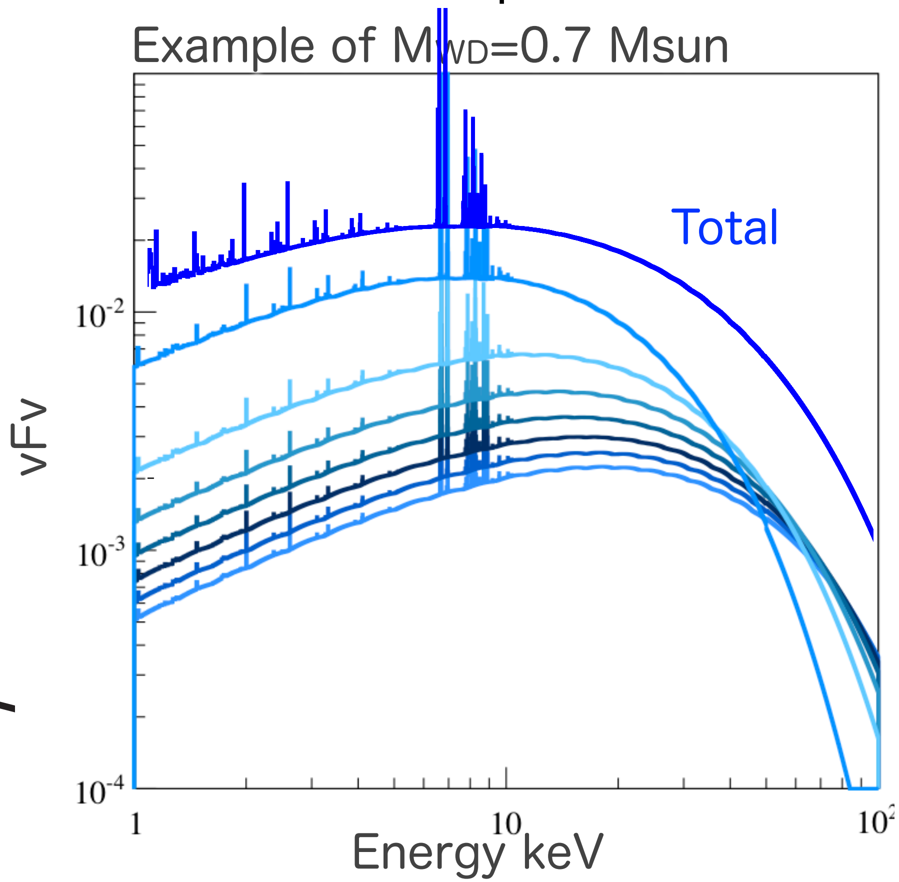

Close-up view of Fe lines

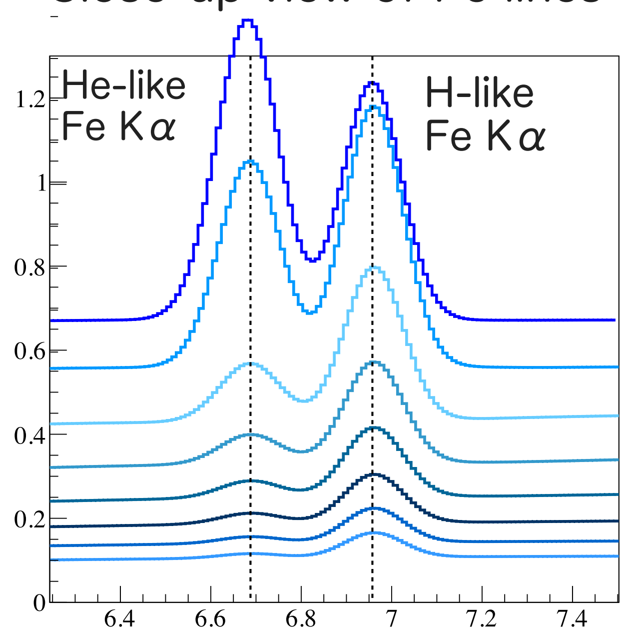

Spectral extraction

- Fluxes of the sources are 1-5×10^{-11} erg cm^{-2} s^{-1} (2-10 keV) ∼ 1 to a few mCrab.
- The XIS clearly resolves three Fe emission lines.
- The HXD measures significant signals up to 40-50 keV.

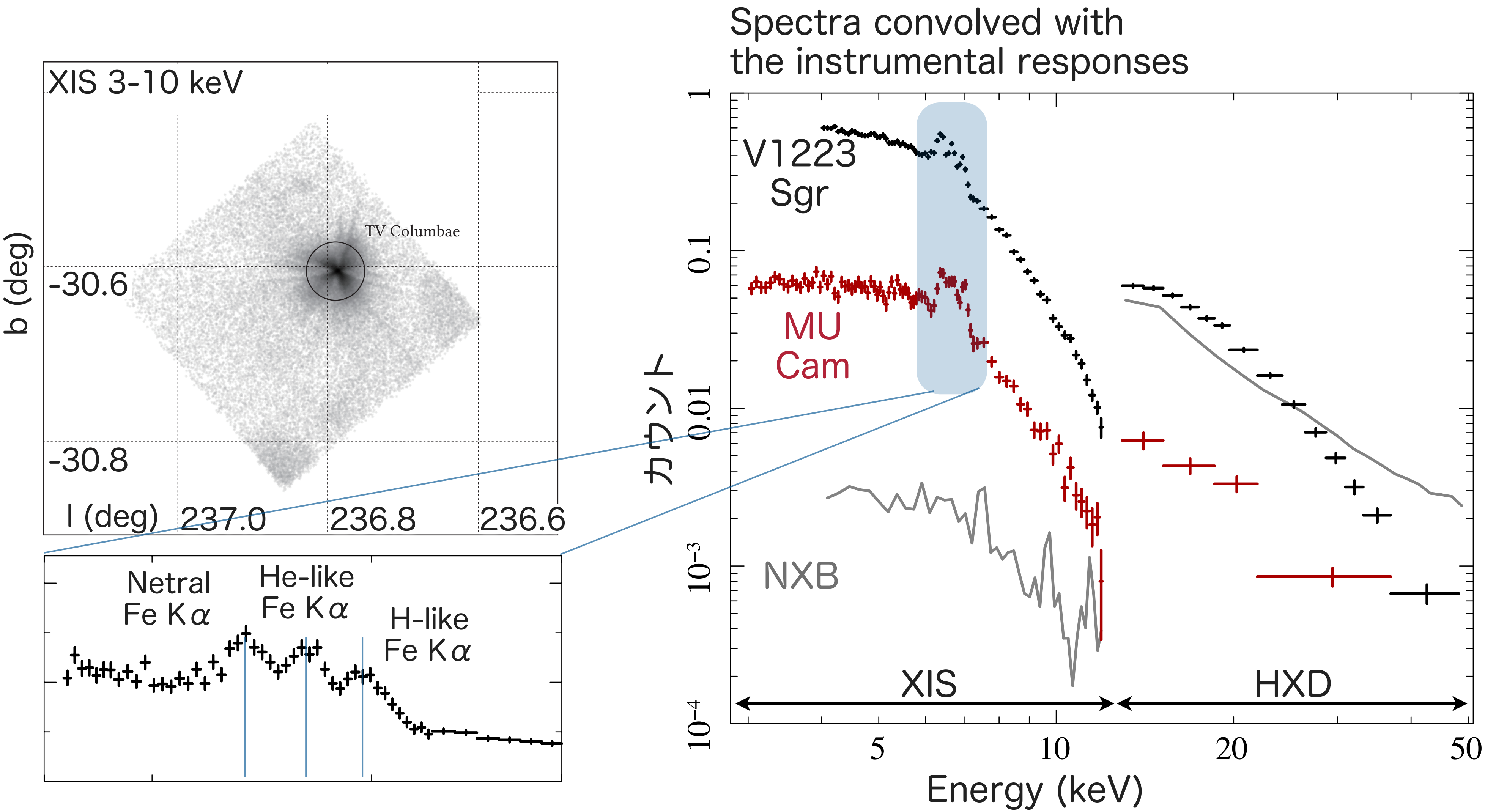

System	$Z_{\rm Fe}$ ($Z_\odot$)	$M_{\rm WD}$ ($M_\odot$)	$kT_{\rm s}$ (keV)	nH[a] 10^{22} cm^{-2}	nH$_{\rm PC}$[b] 10^{22} cm^{-2}	$C_{\rm PC}$[c]	$\chi^2_\nu(\nu)$	$F_{2,10}$[d]	$F_{12,40}$[e]
FO Aqr	$0.10^{+0.02}_{-0.10}$	$0.51^{+0.09}_{-0.04}$	$17.0^{+4.9}_{-2.0}$	$9.54^{+1.38}_{-2.26}$	$398.0^{+204.0}_{-93.5}$	$0.68^{+0.10}_{-0.24}$	1.00(312)	3.73	1.69
					$41.5^{+7.8}_{-8.2}$	1.0 (fixed)			
XY Ari	$0.36^{+0.03}_{-0.03}$	$0.95^{+0.10}_{-0.12}$	$49.9^{+12.4}_{-11.7}$	$9.62^{+0.43}_{-0.36}$	$115.0^{+33.1}_{-19.9}$	$0.42^{+0.06}_{-0.02}$	0.98(321)	1.42	0.58
MU Cam	$0.49^{+0.07}_{-0.06}$	$0.95^{+0.21}_{-0.22}$	$49.9^{+30.8}_{-19.5}$	$5.42^{+1.34}_{-0.98}$	$92.9^{+39.6}_{-22.6}$	$0.57^{+0.06}_{-0.04}$	1.12(318)	0.92	0.37
BG CMi	$0.18^{+0.04}_{-0.03}$	$1.04^{+0.12}_{-0.10}$	$61.0^{+19.8}_{-12.1}$	$6.83^{+1.64}_{-1.93}$	$40.2^{+18.6}_{-11.2}$	$0.46^{+0.10}_{-0.08}$	1.13(318)	2.01	0.71
V709 Cas	$0.16^{+0.04}_{-0.03}$	$1.07^{+0.10}_{-0.15}$	$65.2^{+17.6}_{-18.5}$	$2.83^{+0.48}_{-0.45}$	$101.0^{+22.9}_{-14.2}$	$0.46^{+0.03}_{-0.02}$	1.05(321)	3.63	1.18
TV Col	$0.41^{+0.04}_{-0.03}$	$0.91^{+0.09}_{-0.08}$	$45.7^{+10.0}_{-7.4}$	$4.48^{+0.88}_{-1.06}$	$45.8^{+16.9}_{-12.1}$	$0.39^{+0.05}_{-0.05}$	1.11(321)	4.67	1.44
TX Col	$0.41^{+0.09}_{-0.09}$	$0.80^{+0.27}_{-0.15}$	$35.8^{+29.5}_{-10.8}$	$1.75^{+1.64}_{-1.75}$	$32.4^{+22.4}_{-14.7}$	$0.41^{+0.14}_{-0.13}$	1.23(186)	1.24	1.12
YY Dra	$0.59^{+0.07}_{-0.06}$	$0.93^{+0.15}_{-0.15}$	$47.8^{+19.0}_{-13.6}$	$0.00^{+0.69}_{-0.00}$	$37.5^{+51.7}_{-25.8}$	$0.18^{+0.08}_{-0.08}$	0.98(318)	3.37	0.70
PQ Gem	$0.17^{+0.04}_{-0.03}$	$1.09^{+0.09}_{-0.13}$	$68.3^{+16.6}_{-17.3}$	$2.91^{+1.25}_{-2.09}$	$46.6^{+21.0}_{-16.6}$	$0.43^{+0.10}_{-0.06}$	1.14(303)	2.21	0.66
EX Hya[g]	$0.55^{+0.04}_{-0.03}$	$0.43^{+0.02}_{-0.02}$	$13.1^{+0.9}_{-0.9}$	$0.81^{+0.23}_{-0.19}$	$99.6^{+13.5}_{-10.6}$	$0.42^{+0.04}_{-0.05}$	1.31(316)	8.49	1.32
NY Lup	$0.42^{+0.03}_{-0.02}$	$1.26^{+0.04}_{-0.03}$	$106.1^{+14.9}_{-9.0}$	$8.60^{+0.88}_{-0.96}$	$202.0^{+35.3}_{-28.4}$	$0.55^{+0.04}_{-0.03}$	1.16(251)	2.80	1.22
V2400 Oph	$0.25^{+0.03}_{-0.03}$	$0.66^{+0.05}_{-0.06}$	$25.6^{+3.4}_{-3.7}$	$1.93^{+0.75}_{-1.20}$	$302.0^{+65.5}_{-46.9}$	$0.58^{+0.07}_{-0.09}$	0.92(319)	4.61	1.55
					$38.4^{+12.8}_{-11.9}$	1.0 (fixed)			
AO Psc	$0.46^{+0.08}_{-0.04}$	$0.63^{+0.07}_{-0.03}$	$23.7^{+4.6}_{-1.8}$	$2.37^{+1.53}_{-2.37}$	$24.9^{+8.4}_{-8.4}$	$0.51^{+0.16}_{-0.12}$	1.18(317)	4.31	1.04
V1223 Sgr	$0.27^{+0.01}_{-0.02}$	$0.79^{+0.04}_{-0.04}$	$35.0^{+3.3}_{-3.1}$	$9.91^{+0.65}_{-0.61}$	$201.0^{+25.9}_{-9.9}$	$0.50^{+0.03}_{-0.02}$	1.12(252)	8.29	3.49
RX J2133	$0.30^{+0.04}_{-0.03}$	$0.83^{+0.13}_{-0.10}$	$38.3^{+12.8}_{-7.9}$	$12.50^{+1.47}_{-1.76}$	$330.0^{+64.6}_{-50.1}$	$0.62^{+0.05}_{-0.04}$	1.22(194)	2.04	4.57
IGR J17303	$0.23^{+0.04}_{-0.04}$	$1.24^{+0.06}_{-0.39}$	$100.0^{+21.1}_{-59.9}$	$5.21^{+0.49}_{-0.46}$	$278.0^{+34.5}_{-27.2}$	$0.74^{+0.03}_{-0.02}$	1.19(320)	1.79	1.01
IGR J17195	$0.32^{+0.04}_{-0.04}$	$0.94^{+0.11}_{-0.15}$	$48.9^{+13.5}_{-13.9}$	$2.98^{+0.55}_{-0.54}$	$101.0^{+36.8}_{-10.7}$	$0.42^{+0.07}_{-0.04}$	0.95(321)	3.48	1.09

WD mass spectrum

- Estimated M_{WD} values spread over 0.4-1.2 Msun.
  The average and std.dev. is 0.88±0.24 Msun.
  c.f. averaged mass of isolated WD of 0.59±0.02 Msun (Kepler+07).
  - Effect of mass accretion? Just selection bias of our samples (probably)?
- No significant difference is observed when compared with a mass spectrum of non-magnetic CVs (Ritter & Kolb 2003).
- Our mass estimates do not contradict with optical/IR kinematic estimates within errors (although data are quite small).

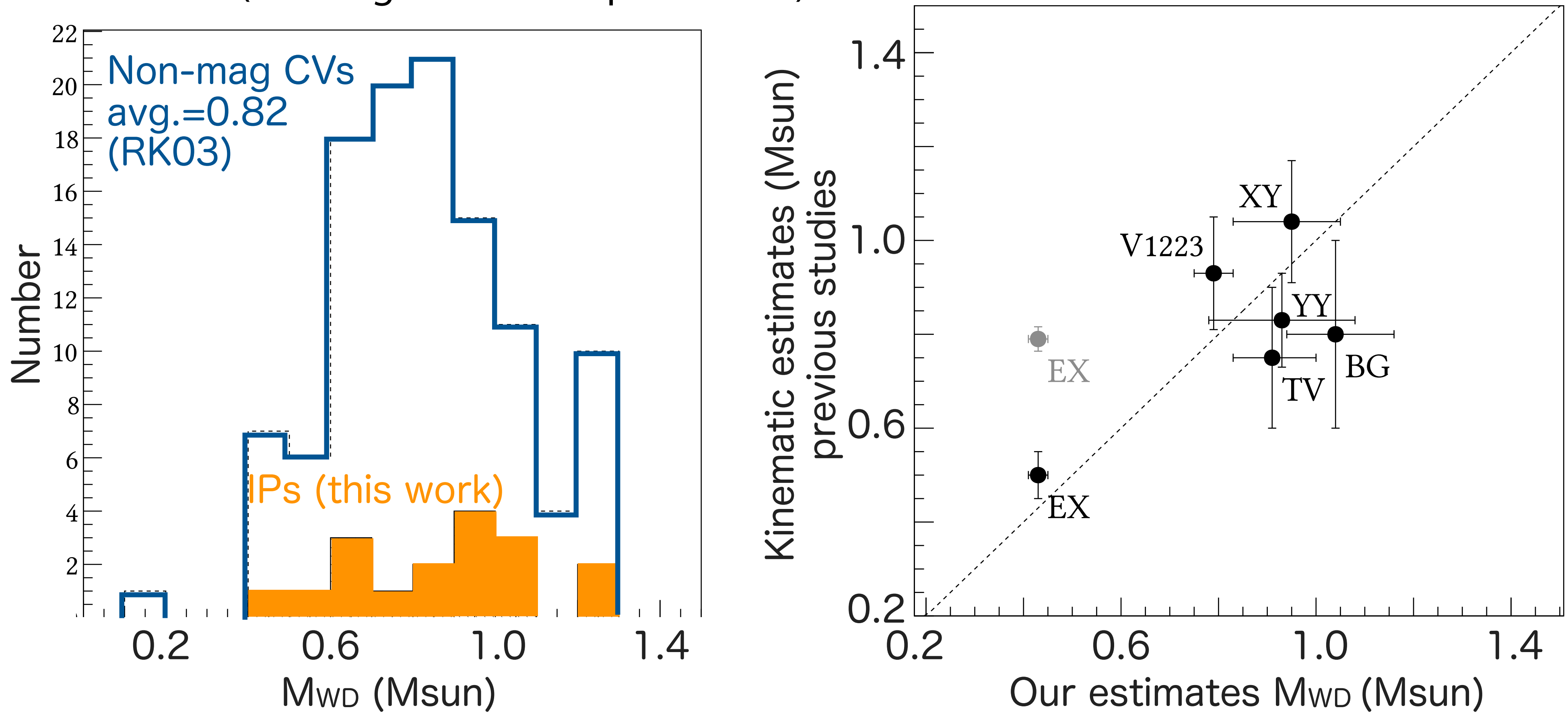

Comparison with previous X-ray studies

- Suleimanov+05 (RXTE; 3-100 keV) ← Fe lines are not used (unresolvable)
- Brunschweiger+09 (Swift; 15-60 keV) ← Only measures 16-60 keV
- We do not see strong correlations between our results and those of the previous reports. In lower masses, our masses are somewhat consistent with those by Suleimanov+05. This is because spectral cutoffs are clearly seen in these cases.

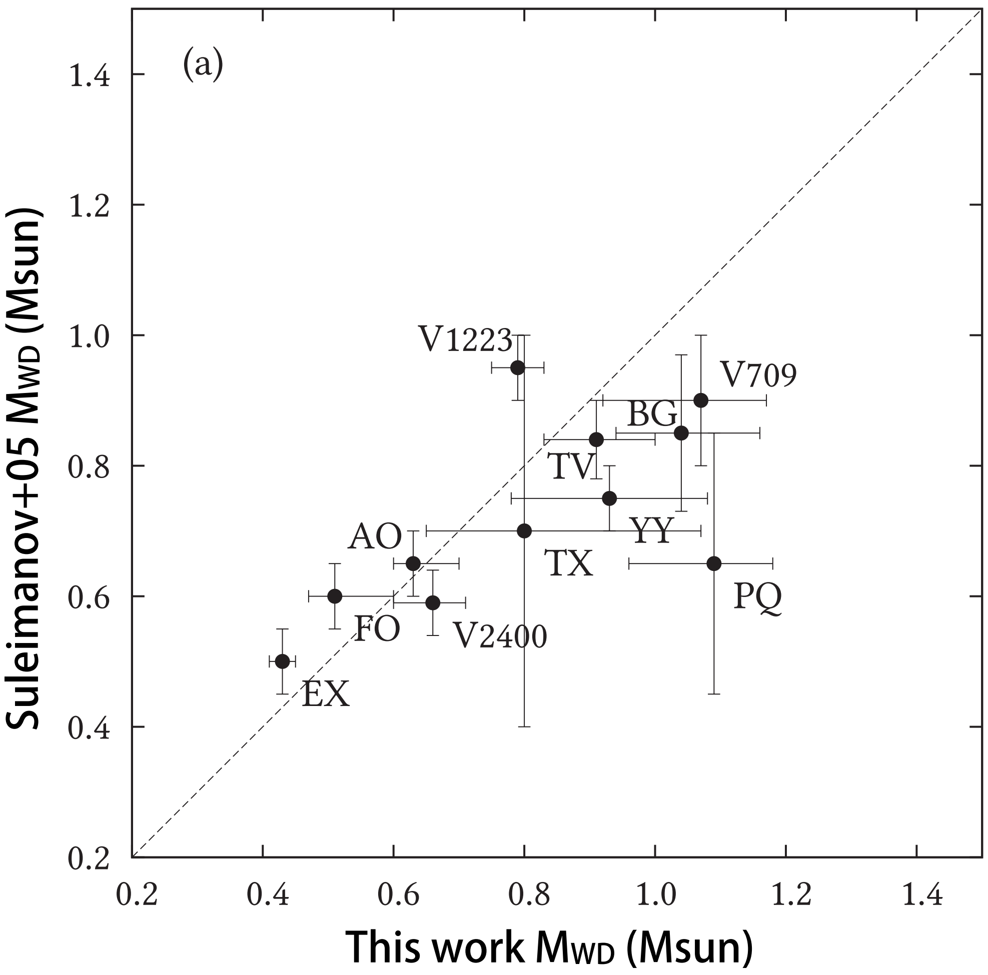

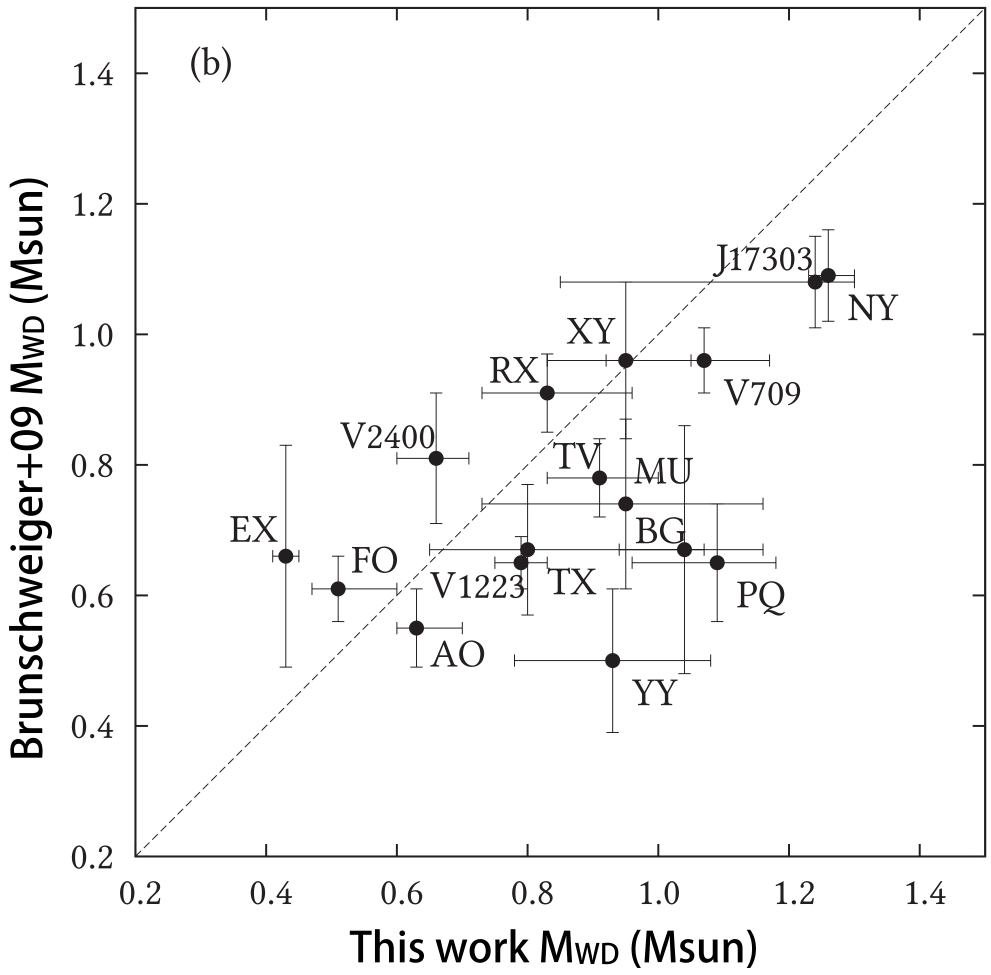

Table 6.1: *Suzaku* observations of the Galactic center analyzed in the present study.

Region 1								
	Obs. ID[a]	Coordinate[b]		Start time	Exposure[c]		Count rate[d]	
		l	b	UT	XIS	PIN	XIS	PIN
1	501053010	−1.83	−0.00	2006-10-10 21:18:59	21.9	19.9	0.49	0.07
2	503014010	−2.10	−0.05	2008-09-18 04:46:49	55.4	51.2	0.36	0.05
3	503015010	−2.35	−0.05	2008-09-19 07:33:05	56.8	52.8	0.38	0.04
4	503016010	−2.60	−0.05	2008-09-22 06:47:49	52.2	49.3	0.36	0.03
5	503017010	−2.85	−0.05	2008-09-23 08:08:10	51.3	48.6	0.33	0.04
6	503021010	−1.62	0.20	2008-10-04 03:44:03	53.8	49.6	0.49	0.07
7	503076010	−1.50	0.15	2009-02-24 17:04:51	52.9	43.8	0.55	0.07
8	503077010	−1.70	0.14	2009-02-26 01:01:00	51.3	43.7	0.48	0.07
9	504001010	−1.47	−0.26	2010-02-26 09:15:00	51.2	42.2	0.41	0.05
10	504002010	−1.53	−0.58	2010-02-27 16:14:41	53.1	46.6	0.35	0.04
11	504003010	−1.45	−0.87	2010-02-25 04:33:17	50.9	41.3	0.39	0.02
12	504090010	−1.49	−1.18	2009-10-13 04:17:20	41.3	35.0	0.40	0.03
				Total Exposure	592.1	524.0		

Region 2								
	Obs. ID[a]	Coordinate[b]		Start time	Exposure[c]		Count rate[d]	
		l	b	UT	XIS	PIN	XIS	PIN
1	502004010	0.17	−1.00	2007-10-10 15:21:17	19.9	18.8	0.90	0.05
2	502059010	−0.00	−2.00	2007-09-29 01:40:51	136.8	110.5	0.70	0.02
3	503081010	0.03	−1.66	2009-03-09 15:41:50	59.2	57.6	0.98	0.01
4	504050010	0.10	−1.42	2010-03-06 03:55:37	100.4	80.5	1.21	0.02
5	504088010	−0.00	−0.83	2009-10-14 11:30:56	47.2	32.6	0.87	0.05
6	504089010	−0.05	−1.20	2009-10-09 04:05:59	55.3	40.2	1.08	0.02
				Total Exposure	418.8	340.2		

Correlation of GRXE and NIR

- Revnivtsev+06 reported nice correlation between the surface brightness of the GRXE and the NIR diffuse emission using RXTE Galactic plane scan data.
- Since NIR surface brightness traces the stellar density, the GRXE origin was suggested to have connection with it (i.e. stellar origin).
- The present Suzaku data also confirms this correlation.

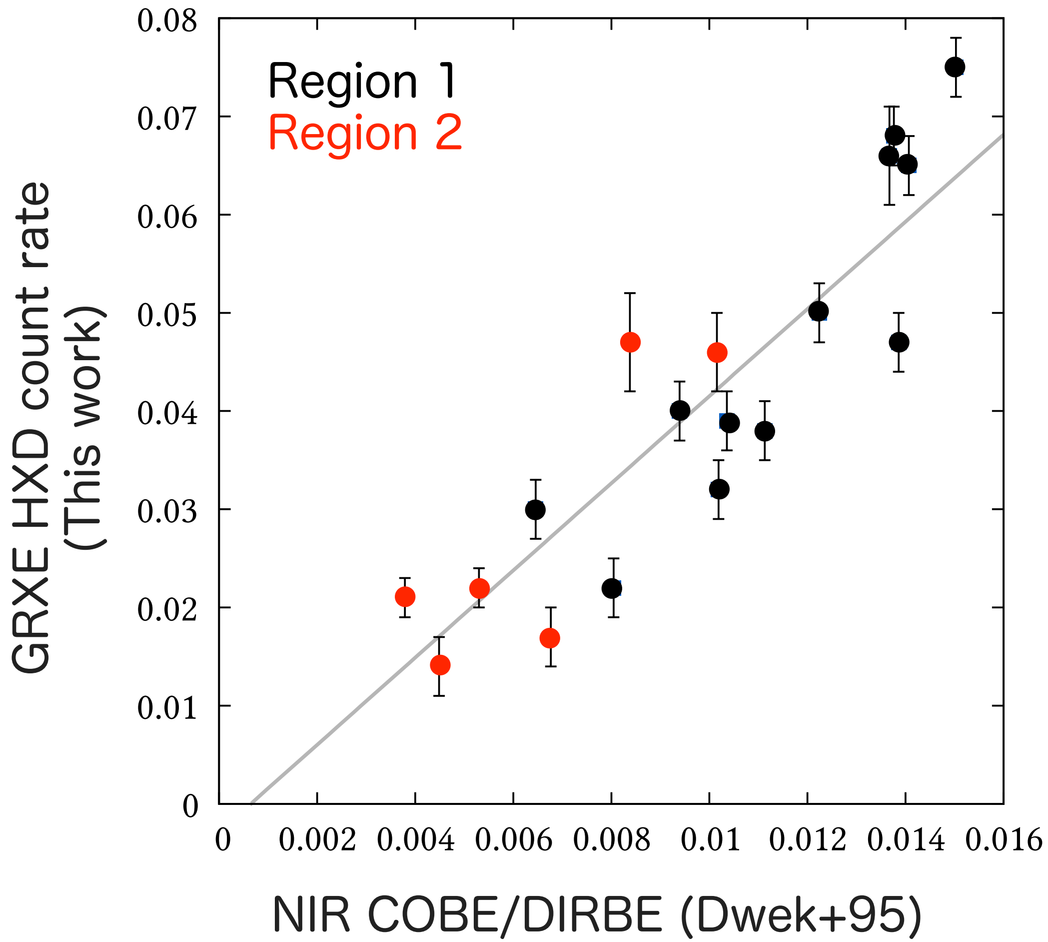

The X-ray observatory ASTRO-H (2014-)

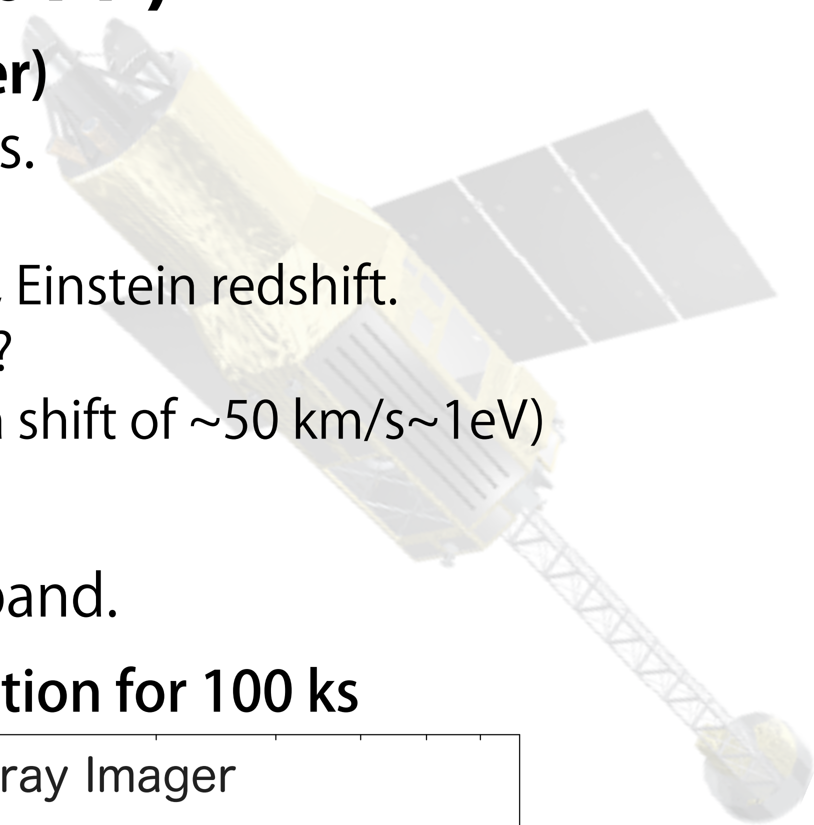

Soft X-ray Spectrometer (X-ray micro-calorimeter)

~6 eV resolution (FWHM) at Fe K emission lines.

→ Resolves the fine structures.

→ Direct measurements of plasma density, velocity, Einstein redshift.

→ Does the GRXE have red-shifted neutral Fe K line?

(if emitted from reflection from the WD surface, a shift of ~50 km/s~1eV)

Hard X-ray Imager with a collection mirror

High statistics and imaging in the hard X-ray band.

Simulation of the IP TV Col observation for 100 ks